

No. 16

**OCEAN RESOURCES INVESTIGATION
IN THE SEA AREA OF CCOP/SOPAC
REPORT ON THE JOINT BASIC STUDY
FOR THE DEVELOPMENT OF RESOURCES**

(VOLUME 1)

SEA AREA OF COOK ISLANDS

February 10, 1986

**JAPAN INTERNATIONAL COOPERATION AGENCY
METAL MINING AGENCY OF JAPAN**

M P N
C R (5)
86-31

OCEAN RESOURCES INVESTIGATION
IN THE SEA AREA OF CCOP/SOPAC

SAE AREA OF COOK ISLANDS
(VOLUME 1)

February 1986

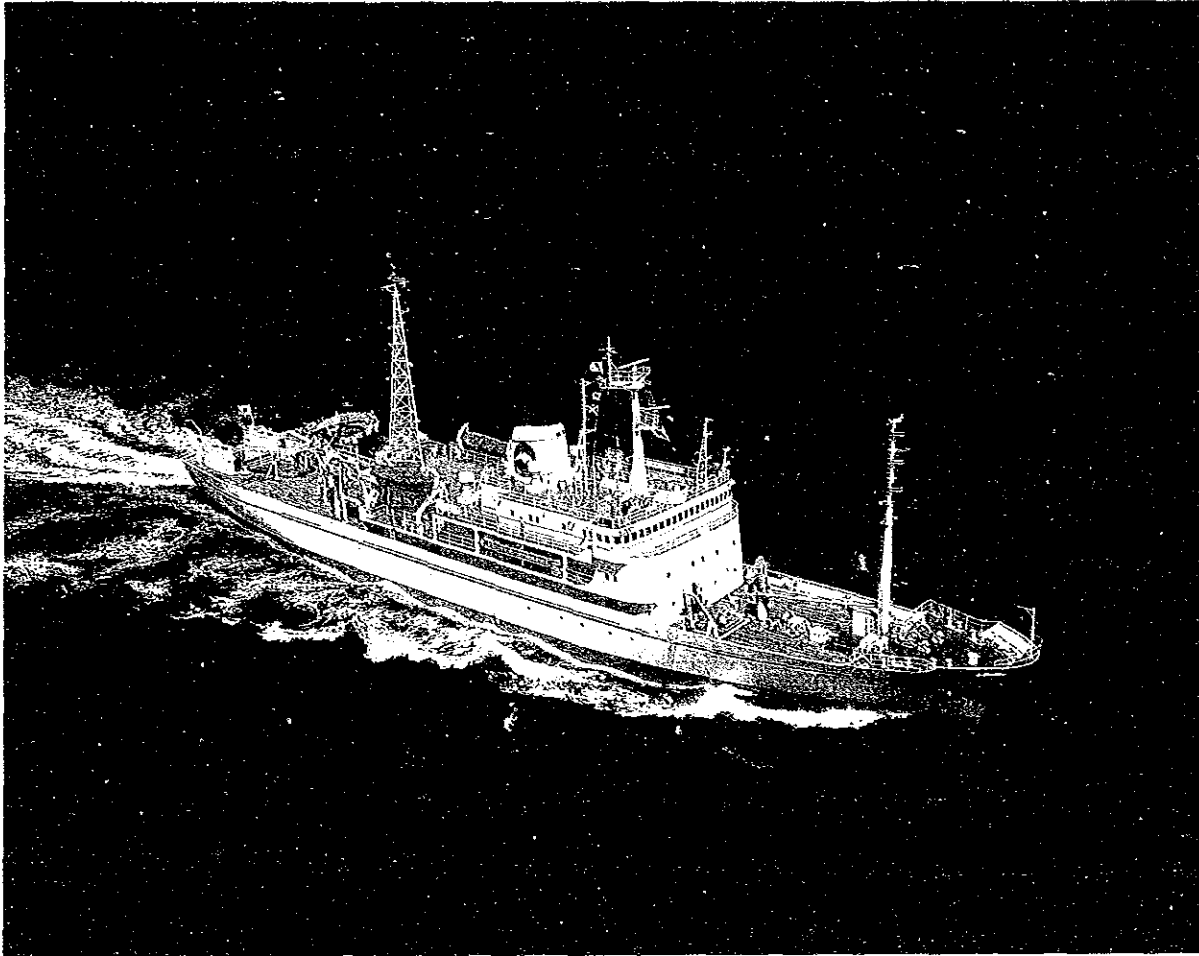
LIBRARY

JICA LIBRARY



1029153[2]

国際協力事業団		
受入 月日	'86. 8. 20	200
登録 No.	15201	65.8
		MPN



Hakurei-Maru No.2, Marine Geological Survey Vessel



LOCATION MAP OF THE SURVEY AREA

PREFACE

In response to the request of the Committee for Co-ordination of Joint Prospecting for Mineral Resources in the South Pacific Offshore Areas (CCOP/SOPAC), the Government of Japan decided to conduct different studies relating to mineral prospecting such as a geological study in order to confirm the mineral resources potential on the deep ocean bottom of the offshore region of the Committee's member countries and consigned performance of the survey to the Japan International Cooperation Agency (JICA).

For the reason that essential of the above-mentioned survey belonged to the professional matters consisting of geological and mineral prospecting studies, the JICA has commissioned the Metal Mining Agency of Japan (MMAJ) to execute the survey.

The survey will be undertaken over a five year period starting from the financial year of 1985. In 1985 the first year, the MMAJ, taking the exclusive economic zone of the Cook Islands as the sphere of the survey, sent the Hakurei Maru No. 2, a research vessel especially commissioned for prospecting mineral resources on the deep ocean bottom, to the sites of the survey from September 23, 1985 until October 30, 1985, and finished research activities on schedule, thanks to the cooperation of the Cook Islands.

The present report sums up the results of the survey accomplished in the first year.

At the end, we wish to tender our sincere thanks to all the persons concerned, especially of the Secretariat of CCOP/SOPAC, the Self-Governing Administration of the Cook Islands and also of the Ministry of Foreign Affairs, the Ministry of International Trade and Industry, the Japanese Embassies in Fiji

and New Zealand, and as well as the private Companies that willingly collaborated with us.

February, 1986

Japan International Cooperation Agency

President Keisuke ARITA

Metal Mining Agency of Japan

President Masayuki NISHIIE

SUMMARY

Pursuant to the request of the Committee for Co-ordination of Joint Prospecting for Mineral Resources in South Pacific Offshore Area (CCOP/SOPAC), with a view to confirming the mineral resources potential on the deep ocean bottom in the exclusive economic zone of the Committee's member countries, we proceeded with the survey.

The results of the studies are summarized as follows:

1) Outline of the survey

The survey areas in the 1985 financial year corresponds to the sea areas of approximately 85,000 km² contained by the lines 6°30' - 8°30'S; 155°00' - 159°30'W.

(1) Methods of the survey

1 Sampling

For sampling of the manganese nodules and bottom materials, the samplers FG (Free Fall Grab) and SC (Spade Corer) were used. In these cases, the samplers were equipped with a single exposure deep-sea camera in order to observe the sampling points, while samples were taken simultaneously.

2 Sea bottom observation

For observing the distribution situation of manganese nodules, the continuous deep-sea camera(CDC) was used. A single exposure deep-sea camera was also used in order to observe the sea bottom conditions at the sampling points.

3 Echo sounding prospection

For the echo sounding prospection, the following are the equipments used: PDR (Precision Depth Recorder) to draw up the topographical maps; SBP (Sub-bottom profiler) to measure the acoustic stratigraphy; and MFES (Multi Frequency Exploration System) to investigate abundance of manganese nodules.

(2) Survey precision

For the sake of sampling accuracy, the primary stage survey was set up with the sampling stations' intervals on a 42.4 nautical mile grid.

The secondary stage survey was proceeded in the selected areas where the abundance of manganese nodules was confirmed to be more than 5 kg/m² by the primary stage, with the sampling stations' intervals on a 21.2 nautical mile grid covering the middle points of the sampling stations of the primary stage.

During the secondary stage, Sea bottom observation by CDC was also carried out at intervals of 5.3 and 1.33 nautical miles along the observation lines selected to cross the most abundant sampling stations. Echo sounding prospection was carried out on the track lines connecting the stations by the shortest distance. Moreover, in case of neccessity, supplementary echo soundings were added on the north-south and east-weat lines.

(3) Survey amount

At the primary stage survey, sampling was executed on 20 stations and at the secondary on 18 stations. With 3 samplings at every stations, the total number of samplings came to 114.

Photographing by CDC covered some 65 nautical miles of the track lines in total, and the observation stations came to 41 and the photos of sea bottom to 168.

Acoustic soundings such as PDR, SBP, MFES covered the length of about 2,660 nautical miles in total respectively.

2) Outline of the survey results

(1) Sea floor topography

Roughly speaking, the 157° 30'W longitudinal line makes a border line between the western part having a trend of deepening westwards and the eastern part getting shallower estwards. The

eastern part demarcated by the 159°W presents an almost plain bottom. Within this part, isolated summits of sea knolls and sea mounts are dispersed along the latitudinal line 7° 30'S and isolated sea mounts with a relative height of 1,200m were recognized around the position 7° 30'S: 157° 30'W.

The western part demarcated by 159° W corresponds to the outside edge of the Manihiki plateau which covers an extensive area to the western areas, and presents a complex and intensively undulated topography.

- (2) Distribution of the manganese nodules in the surveyed areas was ascertained, in general, to be higher to the west of the 158° W longitudinal line and lower to the east.

The following 3 sites were confirmed to indicate an abundance of more than 5 kg/m²:

- ① 85-A: External margin of Manihiki plateau
surface: About 6,500 km²
- ② 85-B: insular area around the position 7° 30'S: 158° 30'W
surface: about 800 km²
- ③ 85-C: insular area around the position 8° 30'S: 158° 30'W
surface: about 400k m²

These sea areas' floors are quite undulated and their depth measures some 5,100 - 5,600m. Exposure ratio of the manganese nodules is rather high. Though manganese nodules were found throughout almost all the surveyed areas, more abundant on the sea mounts or sea knolls generally. Where the sea depth is less than 5,000m, manganese nodules showed the platy, crust-like or massive rock-like ones in morphology. And in rare cases, it was observed that basement rock was exposed directly.

(3) Bottom materials

The sea bottom of almost all surveyed areas is covered with brown clay. Only a small amount of calcareous clay was observed near the summits of sea mounts or sea knolls where the sea depth is less

than 5,000m. Also, in extremely rare cases, clay rich in zeolite was observed within the areas of brown clay.

On the basis of the present survey data, the relationship between the bottom materials and the manganese nodules could not be confirmed.

3) Grade distribution and distribution of metal quantity of manganese nodules

As for the grade and distribution of metal quantity of manganese nodules in the surveyed sea areas, the following regularity was ascertained:

(1) Grade distribution

Concerning the 3 elements of nickel, copper and cobalt mainly that compose the manganese nodules, the following was observed:

- ① In the whole surveyed sea areas, Ni grade is 0.74%, Cu grade 0.51% and Co grade 0.28%.
- ② Concerning the sites of the surveyed sea area where abundance is more than 5kg/m^2 , Ni and Cu grades decrease, while the Co grade goes up as follows:
Ni: 0.44%, Cu: 0.27% and Co: 0.39%.
- ③ As for the sites where abundance is more than 7.5kg/cm^2 , Ni and Cu Grade are found at the same level as in the sites where the abundance is more than 5kg/cm^2 , however the Co grade goes up to 0.43%. Therefore, the surveyed sea areas could be considered as sites where the Co grade is higher.

(2) Distribution of metal quantity

The distribution quantity per unit area of the nickel, copper, and cobalt which are the 3 significant components of manganese nodules were confirmed as follows:

- ① The extent of the bottom surface bearing a nickel metal quantity of more than 20g/m^2 came to about $7,500\text{km}^2$ and its average metal quantity was 29.2kg/m^2 .
- ② The extent of the bottom surface bearing a copper metal

quantity of more than 20 g/m² came to about 630 km² and its average metal quantity was 23.2 kg/m².

- ③ The extent of the bottom surface bearing a cobalt metal quantity of more than 10 g/m² came to about 8,340 km² and its average metal quantity was 29.0 kg/m².

CONTENT

Chapter 1. Forward	1
Chapter 2. Main Points of the Survey	2
2-1 Title of the Survey	2
2-2 Sea Areas of the Survey	2
2-3 Objectives of the Survey	2
2-4 Period of the Survey	3
2-5 Participants in the Survey	3
2-6 Apparatus and Equipment for the Survey	4
1) Vessel position indicator	4
2) Echo sounder	4
3) Exploring equipment for mineral resources in the deep-sea beds	4
(1) MFES	4
(2) CDC	4
(3) Deep-sea camera	4
4) Sampling apparatus	5
5) Analyzing equipment	5
6) Data processing system	5
Chapter 3. Methods of the survey	6
3-1 Numbering of the Track Lines, Sampling Stations and Sampling Points	6
3-2 Vessel Positioning	9
3-3 Sea Floor Topography	10
3-4 Superficial Sediments	10
3-5 Research on Manganese Nodules by Means of MFES	11
3-6 Sampling by Means of FG and SC	11
3-7 Processing, Analyzing and Storing of Samples	14
3-8 Sea Bottom Observation by Means of CDC	22
3-9 Evaluation of the Grab Operations by FG Sampler and of Sample Collecting Accuracy	22
3-10 Processing and Analyzing of the Survey Data	24
1) Surveying data and their processing	25
2) Analyzing of the survey data	28

Chapter 4. Results of the Survey	28
4-1 Survey Achievements	28
4-2 Sea Floor Topography	30
1) Classification of sea floor topography	30
2) Characteristics of sea floor topography	31
3) Local sea floor topography	31
4-3 Superficial Sediment	34
1) Classification of SBP records	34
2) Distribution of SBP types	39
3) Thickness and its distribution of upper transparent layer in SPB profiles	42
4-4 Research on Manganese nodules by means of MFES	43
1) Affecting factors on MFES	43
2) Estimation of manganese nodules by means of MFES	52
4-5 Bottom Materials	54
1) Classification of bottom materials	54
2) Properties of bottom sediments	55
3) Composing minerals of bottom materials	57
4) Chemical composition of bottom materials	60
5) Rocks of bottom materials	60
6) Distribution of bottom materials	61
7) Identification of microfossils in bottom sediments	63
4-6 Sea bottom Observation	70
1) Observation by CDC	70
2) Observation by means of deep-sea camera	75
4-7 Assaying	79
1) Inspection on the bias	79
2) Examination of the results	80
4-8 Manganese nodules	82
1) Physical properties (morphology and granular size - characteristics by external appearance - water content)	82
2) Chemical properties (5 principal components - total analysis - micro-analysis - chemical properties of section)	88

3) Mineral properties (X-ray diffraction - microscopic observation)	99
4) Distributional characteristics of manganese nodules	108
(1) Morphology distribution of manganese nodules	108
(2) Size distribution of manganese nodules	108
(3) Size and morphology	111
(4) Local topography and morphology	111
(5) SBP types and morphology	111
(6) Bottom materials and morphology	114
5) Sea bottom situation and abundance	114
(1) Morphology of the manganese nodules and abundance	114
(2) Sea floor topography and abundance	114
(3) SBP types and abundance	118
(4) Upper transparent layers and abundance	118
(5) SBP records and embedding ratio of the manganese nodules	121
(6) Bottom materials and abundance	122
4-9 Bearing Situation of Manganese Nodules	124
1) Abundance of the manganese nodules	124
2) Grade distribution	124
3) Distribution of metal quantity (Ni, Cu, Co)	126
Chapter 5. Summary	129
1) Conclusion	129
2) Grade distribution and metal quantity distribution of manganese nodules	131
3) Proposal for the next financial year	132
List of the inserted tables	
Table 4-1-1 List of the Survey Achievements	28
Table 4-2-1 Classification of Sea Floor Topography	30
Table 4-5-1 Classification Criteria of Bottom Sediments	54
Table 4-5-2 Results of X-ray Diffraction Analysis of Bottom Materials	59
Table 4-5-3 Chemical Composition of the Bottom Materials	59
Table 4-5-4 List of the Collected Radiolarias (Part 1)	68
Table 4-5-5 List of the Collected Radiolarias (Part 2)	69

Table 4-7-1	Estimated values of a, b and correlation coefficients	81
Table 4-7-2	Examination of the bias and the accidental errors by Regression Analysis	81
Table 4-7-3	Bias and Accidental Errors Resulting from Inspection of the Difference of Average Values	81
Table 4-8-1	Physical Properties Associated with Morphology of Manganese nodules	84
Table 4-8-2	Chemical Properties of Manganese Nodules	92
Table 4-8-3	Morphology and Chemical Properties of Manganese Nodules	92
Table 4-8-4	Size and Chemical Properties of Manganese Nodules	95
Table 4-8-5	Sea Floor topography and Chemical Properties of Manganese Nodules	96
Table 4-8-6	Bottom Sediments and Chemical Properties of Manganese Nodules	96
Table 4-8-7	Chemical Composition of Manganese Nodules	98
Table 4-8-8	Chemical Compositional Difference Between Surface and Inner Part Nodules	100
Table 4-8-9	Results of X-ray Diffraction Analysis of the Manganese Nodules	104
Table 4-8-10	Relation Between Regional Sea Floor Topography and Abundance of Manganese Nodules	114
Table 4-8-11	Relation Between Local Sea Floor Topography and Abundance of Manganese Nodules in Plain Province	117
Table 4-8-12	Relation Between Local Sea Floor Topography and Abundance of the Manganese Nodules in Hilly Province	117
Table 4-8-13	Relation Between Thickness of Upper Transparent Layers by SBP and Embedding Ratio	121
Table 4-8-14	Relation Between SBP Type and Embedding Ratio of Manganese Nodules	122

List of the inserted figures

	Location map of the survey areas	
Figure 3-1-1	Explanation on Numbering of Sampling Stations and Sampling Points	7
Figure 3-1-2	Numbering of the Areas in the Surveyed Sites	7

Figure 3-6-1	Distribution Density of Sampling Stations	12
Figure 3-6-2	Explanation on the Setting Order of Three Samplers at a Sampling Station	13
Figure 3-7-1	Processing and Assaying Flowsheet of Samples (No. 1)	15
Figure 3-7-2	Processing and Assaying Flowsheet of Samples (No. 2)	16
Figure 3-7-3	Acoustic Sounding and Processing Flowsheet	17
Figure 3-8-1	Track Lines of Sea Bottom Observation by Means of CDC	18
Figure 3-8-2	CDC Observation Stations	20
Figure 3-9-1	Calculating Criteria of Grab Precision	23
Figure 4-2-1	Explanation on Sea Floor Topography	32
Figure 4-2-2	Section of the Sea Floor Topography	33
Figure 4-3-1	Classification of SBP Records (No. 1)	36
Figure 4-3-2	Classification of SBP Records (No. 2)	37
Figure 4-3-3	Classification of SBP Records (No. 3)	38
Figure 4-3-4	Distribution of SBP Types	40
Figure 4-4-1	Distribution of Weight Coefficient	44
Figure 4-4-2	Distribution of Embedded Type Manganese Nodules	46
Figure 4-4-3	Influence of Embedded Type Manganese Nodules on MFES Measurement	46
Figure 4-4-4	Classification of Sampling Stations into Plain and Hilly Provinces	48
Figure 4-4-5	Relation Between MFES Intensity and Abundance of Manganese Nodules	
Figure 4-4-6	Relation Between MFES Intensity and Abundance of Manganese Nodules in Plain and Hilly Province	49
Figure 4-4-7	Relation Between MFES Intensity and SBP Type	51
Figure 4-4-8	Estimated High Potential Area by MFES Intensity	53
Figure 4-5-1	Smear Slide Photos of Bottom Sediments	56
Figure 4-5-2	Typical Pattern of the X-ray Diffraction of Bottom Sediment and Authigenic mineral	58
Figure 4-5-3	Microscopic Photos of Authigenic Minerals	62
Figure 4-5-4	Distribution of Bottom Materials	64
Figure 4-5-5	Species of the Typical Radiolarian Fossil (No. 1)	65
Figure 4-5-6	Species of the Typical Radiolarian Fossil (No. 2)	66

Figure 4-6-1	Examples of Photos by CDC	76
Figure 4-6-2	Examples of Deep-Sea Bottom Photos and of Re-collected Photos (No. 1)	77
Figure 4-6-3	Examples of Deep-Sea Bottom Photos and of Re-collected Photos (No. 2)	78
Figure 4-8-1	Morphology of Manganese Nodules (No. 1)	85
Figure 4-8-2	Morphology of Manganese Nodules (No. 2)	86
Figure 4-8-3	Morphology of Manganese Nodules (No. 3)	87
Figure 4-8-4	Morphology, Size and Sampling Weight of Manganese Nodules	89
Figure 4-8-5	Frequency Distribution of 5 Principal Components	91
Figure 4-8-6	Scatter Diagram Among Respective Components	93
Figure 4-8-7	Photos of Manganese Nodules Used for Section Analysis	101
Figure 4-8-8	Grade of Respective Section of Manganese Nodules	102
Figure 4-8-9	Photos of Manganese Nodules Used for X-ray Diffraction Analysis	105
Figure 4-8-10	X-ray Diffraction Pattern of the Manganese Nodules	106
Figure 4-8-11	Macro-Photo and Microscopic Photos of Polished Thin Section of Manganese Nodules	107
Figure 4-8-12	Morphology Distribution of Manganese Nodules	109
Figure 4-8-13	Size Distribution of Manganese Nodules	110
Figure 4-8-14	Relation Between Size and Morphology	112
Figure 4-8-15	Relation Between Local Topography and Morphology	112
Figure 4-8-16	Relation Between SBP Type and Morphology	113
Figure 4-8-17	Relation Between Upper Transparent Layer Thickness and Morphology	113
Figure 4-8-18	Relation Between Bottom Sediments and Morphology	115
Figure 4-8-19	Average Abundance by Respective Morphology and Occurrence Ratio by Respective Abundance of Manganese Nodules	116
Figure 4-8-20	Relation Between SBP Type and Abundance of Manganese Nodules	119
Figure 4-8-21	Relation Between Upper Transparent Layer Thickness and Abundance of Manganese Nodules	120
Figure 4-8-22	Average Abundance by Respective Bottom Sediments and Occurrence Ratio by Respective Abundance of Manganese Nodules	123

List of the Annexed Figures

Annexed Figure 1	Tracklines Map	133
Annexed Figure 2	Positions of Sampling Points	134
Annexed Figure 3	Sea Floor Topography	135
Annexed Figure 4	Acoustic Thickness of Upper Transparent Layers by SBP	136
Annexed Figure 5	MFES Intensity Map	137
Annexed Figure 6	Estimated Abundance by CDC Observation	138
Annexed Figure 7	Abundance Map of Manganese Nodules	139
Annexed Figure 8	Ni Grade Map of Manganese Nodules	140
Annexed Figure 9	Cu Grade Map of Manganese Nodules	141
Annexed Figure 10	Co Grade Map of Manganese Nodules	142
Annexed Figure 11	Mn Grade Map of Manganese Nodules	143
Annexed Figure 12	Fe Grade Map of Manganese Nodules	144
Annexed Figure 13	Ni Metal Quantity Map	145
Annexed Figure 14	Cu Metal Quantity Map	146
Annexed Figure 15	Co Metal Quantity Map	147

Annexed Documents

List of the Survey Results

Chapter 1. Forward

In response to the request of the Committee for Co-ordination of Joint Prospecting for Mineral Resources in South Pacific Offshore Areas, we have executed the survey to confirm the deep-sea mineral resources potential in the economic sea areas of the Cook Islands, using the research vessel "Hakurei Maru No. 2" especially commissioned to explore mineral resources on the deep-sea beds and having technical experience and equipment in studying the field of the manganese nodules.

Thanks to good weather, the survey proceeded satisfactorily and were accomplished on schedule.

The details of the survey are as follows.

Chapter 2. Main Points of the Survey

2-1 Title of the Survey

Deep Ocean Mineral Resources Investigation
In the Sea Areas of CCOP/SOPAC
Joint Basic Study for the Development of Mineral Resources in the
Exclusive Economic Zone of Cook Islands.

2-2 Sea Areas of the Survey (cf. Location Map)

Pursuant to the Cooperative Study Programme and its Scope of Work relating to the deep-sea bottom mineral resources in the economic sea areas of CCOP/SOPAC, concluded in July 1985 between the Government of Japan of one part and the Secretariat of CCOP/SOPAC and also the concerned 3 countries (Cook Islands, Tuvalu and Kiribati) of the other part, the sea areas contained in a polygon (surface: approximately 85,000Km²) enclosed by geodesic lines drawn between coordinates numbered in the series listed below were designated as the survey areas:

	Latitude	Longitude
①	6° 30'S	159° 30'W
②	6° 30'S	156° 00'W
③	8° 30'S	156° 00'W
④	8° 30'S	159° 30'W
①	6° 30'S	159° 30'W

2-3 Objectives of the Survey

The objectives of the present survey consisted of confirming the bearing situation of mineral resources distributed on the deep sea bottom of the Cook Islands sea areas and of other related studies.

2-4 Period of the Survey

Survey: September 23, 1985 - October 30, 1985
Analyzing: October 31, 1985 - February 10, 1986

2-5 Participants in the Survey

Japanese side

Negotiation for the agreement

Toshio SAKASEGAWA (Metal Mining Agency of Japan)
Tetsuro KAWAGUCHI (Ministry of Foreign Affairs)
Shoji KUSUDA (Ministry of International Trade and Industry)
Hideyuki UEDA (Japan International Cooperation Agency)
Kaoru HONJO (Metal Mining Agency of Japan)

Supervising at the surveying sites

Toru MIURA (Metal Mining Agency of Japan)
Seizo NAKAO (Geological Survey of Japan)
Yoshiyuki KITA (Metal Mining Agency of Japan)

Members of the surveying team

Chief of the team

Motohide HIROTA (Deep Ocean Resources Development DORD)

Member of the team

Sakiyuki MONONOBE	(idem)
Hiroshi KUSAKA	(idem)
Kohei MAEDA	(idem)
Kiyoshi TONO	(idem)
Taizo MATSUMOTO	(idem)
Masatoshi HOSODA	(idem)
Hisanori TAKAHASHI	(idem)
Kenji SHINOHARA	(idem)
Atsushi SHINDO	(idem)
Hirimitsu SHIMOGAMA	(idem)

Masaki HASHIMOTO	(idem)
Nobuyuki MURAYAMA	(idem)
Ichiro YAMASHITA	(idem)
Masayuki SUZUKI	(idem)

Consigning side

Negotiation for the Agreement

Cruz A. MATOS (Secretariat of CCOP/SOPAC)

Norman GEORGE (Cook Islands)

Babera KIRATA (Republic of Kiribati)

H. E. Feue TIPU (Tuvalu)

Surveying trainee

Teariki RONGO (Cook Islands)

2-6 Apparatus and Equipment used in the Survey

The main apparatus and equipment used in the survey during the current financial year were as follows:

1) Vessel positioning system

(1) Navy navigation satellite system (NNSS); manufactured by MAGNAVOX

2) Echo sounder

(1) Precision depth recorder (PDR), 12 kHz; manufactured by NEC

(2) Sub-bottom profiler (SBP), 3.5 kHz; manufactured by NEC

(3) Narrow beam sounder (NBS), 30 kHz; manufactured by Honeywell ELAC

3) Exploring equipment for mineral resources in the deep-sea beds

(1) Multi-frequency exploration system (MFES); manufactured by Sumitomo Metal Mining

(2) Continuous deep-sea camera system; manufactured by DORD

(3) Deep-sea camera; manufactured by Preussag

4) Sampling apparatus

(1) Suspended type sampler

Spade corer (SC); manufactured by Ocean Instruments

(2) Automatic sinking and re-floating type sampler

Free fall grab (FG); manufactured by Preussag

(3) Mud collector for the free fall grab; manufactured by DOMA

5) Assaying equipment

(1) Preparatory treatment equipment (drying, grinding); manufactured by Yoshida Seisakusho.

(2) Fluorescent X-ray analysis equipment; manufactured by Rigaku Denki.

6) Data processing system

1) Data processing system; manufactured by NEC

Chapter 3. Methods of the Survey

3-1 Numbering of the track lines, sampling stations and sampling points

1) Numbering of the track lines

- (1) Numbering was put on the track lines for acoustic sounding, so that the date and order of working were able to be identified by every cruising unit; for instance, 85S0927A, 85S0927B.

For the night cruising, "N" was added to the end of numbers such as 85S0927N.

For the lines merely between sampling points, "P" (Position) was added such as 85S0927P.

In these cases, "85S" means the financial year of the survey (1985) and the study organization (CCOP/SOPAC-S); "0927" indicates the month of September and the date of 27th, and "A, B" the order of measuring lines on that day.

- (2) Measuring lines for CDC (Continuous deep-sea camera)

The measuring lines are identified by additional numbers such as 85SCDC01, 85SCDC02

2) Numbering of the sampling stations and sampling points

- (1) In the current financial year, "85S" was prefixed to indicate the financial year of the survey (1985) and the study organization (CCOP/SOPAC-S).
- (2) The surveyed sea area was divided in quadrilaterals formed with the longitudinal and latitudinal lines marked at every 1° starting from the origin 1°N : 175°E towards east and south.
- (3) To these quadrilaterals the areas' numbers were designated as shown in the Fig. 3-1-1.

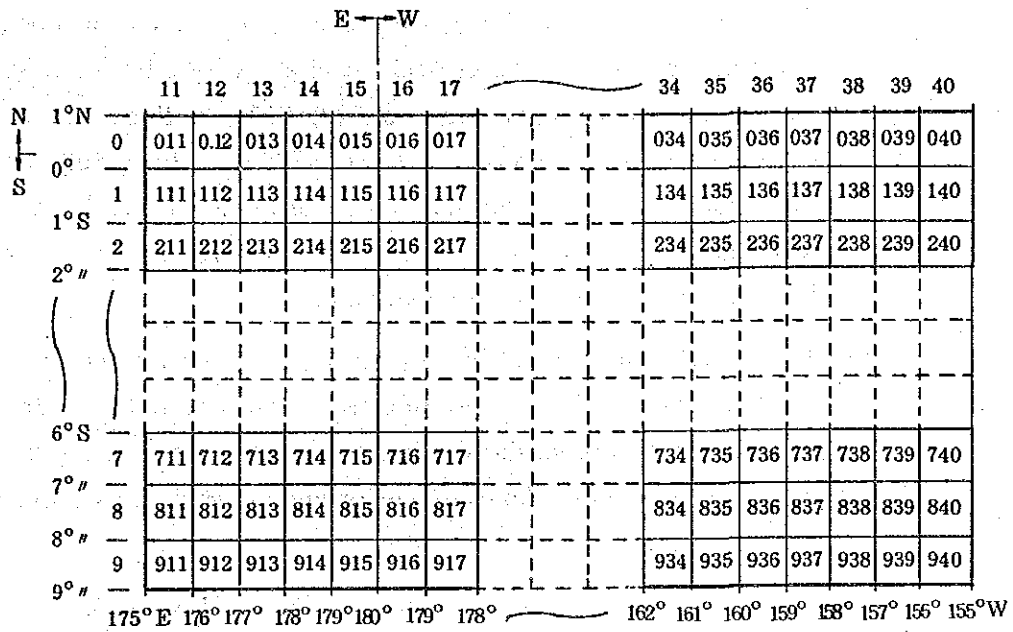


Fig. 3-1-1 Explanation on Numbering of Stations and Sampling Points

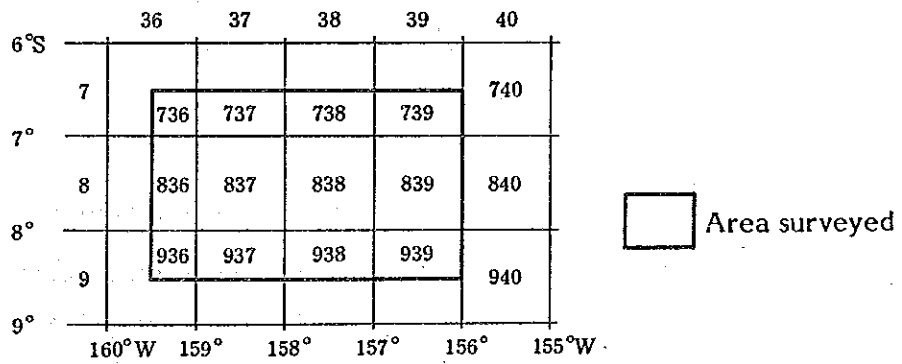


Fig. 3-1-2 Numbering of the Areas in the Surveyed Sites

That is to say, as the Figure shows, the area of north-west extremity was numbered as "011"; and at every advance eastwards, the number progresses such as 012, 013 likewise, at every advance southwards such as 111, 211, 311 Concretely speaking, the figures at the hundred level designate areas in the same latitudinal zone, the figures at the ten level and the one level indicate in the same longitudinal zone.

- (4) The areas' numbers defined in the previous paragraph (3) contain north and west sides of the numbered areas and not east and south sides; in other words, these areas correspond to the fourth quadrant of rectangular co-ordinates, the origin of which is at the north-west extremity.
- (5) The areas surveyed in the current financial year are contained within the quadrilateral formed by the lines connecting successively the points:
 - ① 6°30'S: 159°30'W,
 - ② 6°30'S: 156°00'W,
 - ③ 8°30'S: 156°00'W,
 - ④ 8°30'S: 159°30'W,
 - ① 6°30'S: 159°30'W'

Therefore, the areas' numbers are as shown in the Fig. 3-1-2.

- (6) The sampling that took place in the areas appointed in the previous paragraph (5) and the samples thus collected were numbered with additional figures beginning from "01", after being marked with signs according to the respective sampling methods. From the numbering point of view, the primary survey and the secondary survey were not distinguished.

FG: samples taken by means of the free fall grab

SC: samples taken by means of the spade corer

- (7) Summing up the above-mentioned explanations, the sample number "85S838FG25" signifies the 25th sample collected by means of FG in the area 838, SOPAC in 1985.

3-2 Vessel Positioning

During the survey, all the vessel positions were indicated by "NNSS". The vessel positions determined by the dead reckoning navigation system during the time elapsed from a certain "UP-DATE" *1 to the next "UP-DATE", were corrected by proportional allotment according to this time elapsed; namely, the so-called "corrected positions" were adopted.

The vessel positions as follows were registered in the field notes or in other ways to be utilized for the data processing and analysis to be explained later.

- ① starting and terminating positions on the measuring lines, course alteration points of vessel, positions at every hour of integral number;
- ② samplers' setting positions and their re-collecting positions;
- ③ setting and re-collecting positions of the towing apparatus for observation by CDC, starting and terminating positions of the observation.

All the vessel positions relating to the survey activities were registered in MT with on-line by using the data processing system on board. Also, the corrected vessel positions were printed out by the same system once every minute according to the respective UP-DATE in order to be utilized for filing and analyzing the survey data.

*1 The "UP-DATE" means the moment of determining vessel position 17 minutes after FIX moment of vessel position given by the satellite. (This determined position is a presumed one) During the survey, 4 satellites were available.

3-3 Survey of the Sea Floor Topography

As for the survey of the sea floor topography, fathoming and topographical observation were practiced mainly by means of PDR between the respective stations and between the respective sampling points. Moreover, on the occasion of observation by CDC, research on the sea bottom topography was carried out in the surrounding areas as well as along the track lines.

Fathoming was carried out every 12 seconds; fathoming values indicated by PDR digitizer were registered on MT with the on-line system.

In addition, every 5 minutes, sea depths were recorded by the registered papers of the PDR and with this data, the sea floor topographic maps and other documents were produced.

The survey between the measurement stations was executed generally at the vessel speed of 10 knots, but according to the surveying situation, the vessel speed was accordingly increased or reduced. As for the track lines between sampling points, the vessel speed varied from 3 to 8 knots according to the sampling operation.

3-4 Survey on the Superficial Sediment

The survey of the superficial sediment of the sea bottom was carried out simultaneously with the sea bed survey, by means of SBP (frequency of 3.5 kHz) on all the cruised track lines.

The basic data of the superficial sediment consist of informations such as thickness of transparent layers composing the upper most stratum on the basis of the registered section pattern of SBP and acoustic stratigraphy type, etc.; this information was marked in their cording field notes every 10 minutes and used to draw up the contour map of the superficial sediment thickness and the SBP type distribution map.

3-5 Research on Manganese Nodules by means of MFES

The survey on the bearing situation of manganese nodules by means of MFES was carried out simultaneously with the research on the sea floor topography and the superficial sediment.

The measuring values of MFES were continuously indicated every 48 seconds by calculating data produced by NBS, PDR and SBP, but the moving average of 15 measured values was taken as MFES values of evidence.

The measuring values of MFES were registered in MT by means of an interface with the data processing system and also these basic data as registered on the MFES floppy-disc about every 5 minutes.

3-6 Process of Sampling by means of FG and SC

1) Sampling by FG

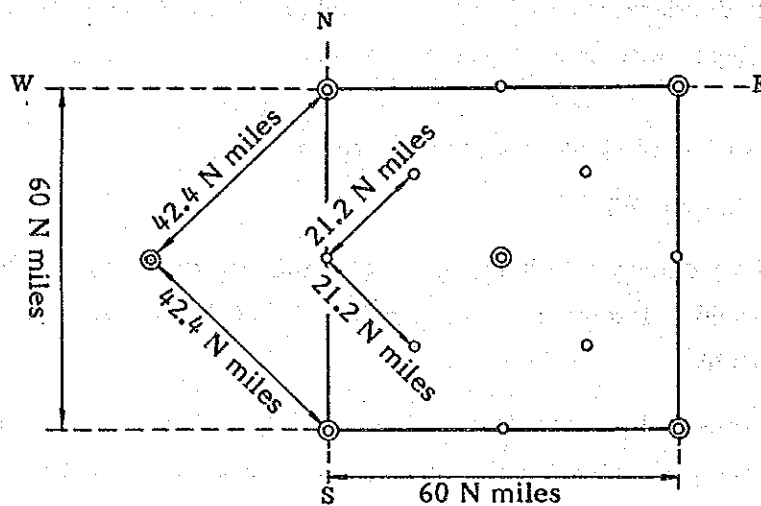
The fundamental chart used for the survey was marked by the sectioning datum lines at every 1° (60 N miles) in latitude and longitude.

As the sampling operations were based upon this chart, the precision of surveying stations for the primary and secondary surveys were chosen as described as follows:

Primary stage: stations for sampling fixed on a 42.4 N mile grid connecting the crossing point of sectioning lines at every 1° (60 N miles) in latitude and longitude to the centre of the section;

Secondary stage: stations covering the middle stations of the primary stage were added and the sampling point interval was reduced to a 21.2 N mile grid.

The above-mentioned scheme is shown in Fig. 3-6-1.



⊙ Primary survey station: 42.4 N mile grid

○ Secondary survey station: 21.2 N mile grid

Notes 1) 60 N miles section correspond to every 1° in latitude and longitude

2) 1 N mile equals to 1.852 km

Fig. 3-6-1 Distribution Density of Sampling Stations

At every surveying station, three samplings were taken and the process is as follows:

The samplers were set down at each apex of the right isosceles triangle whose the southern side centering apex should be located on the given station; the setting down points were considered as sampling points. In other words, sampling was done at every surveying station and then at the two other points respectively 1.4 N miles to the northwest and to the northeast from the station.

From whichever direction the vessel approached the sampling station, it passed through the station once and after confirming the station, it returned to it and set down the first sampler. The order of setting down the 3 point sampling system is illustrated in Fig. 3-6-2.

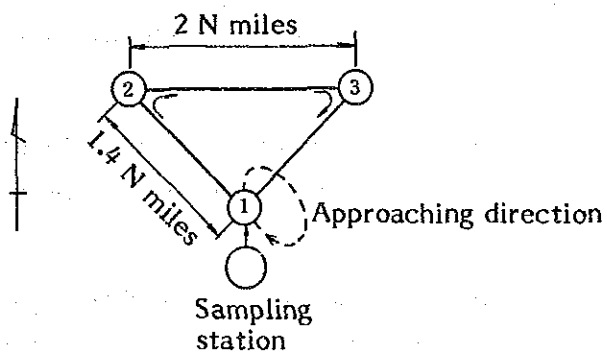


Fig. 3-6-2 Explanation on the Setting Order of Three Samplers at a Sampling Station

3-7 Processing, Analyzing and Storing of Samples

The re-collected samples (manganese nodules and bottom materials) were treated on board on the basis of the processing and analyzing flowsheet of samples by FG and SC shown in the Fig. 3-7-1, -2, -3; also, a part of the samples were taken to the laboratory to be processed for microscopic observation, X-ray diffraction test, complete analysis, micro-analysis, etc., and the rest were kept in storage.

3-8 Observation of the Sea Bottom by means of CDC

With a view to observe minutely the manganese nodules bearing on the deep ocean floor and the sea bottom situation, the sea bottom observation by means of CDC was carried out.

1) Selection of the track lines for CDC

In selecting the observation lines for CDC within the sea areas of the present survey where the secondary survey had been achieved, the fundamental conditions such as the following were taken into consideration:

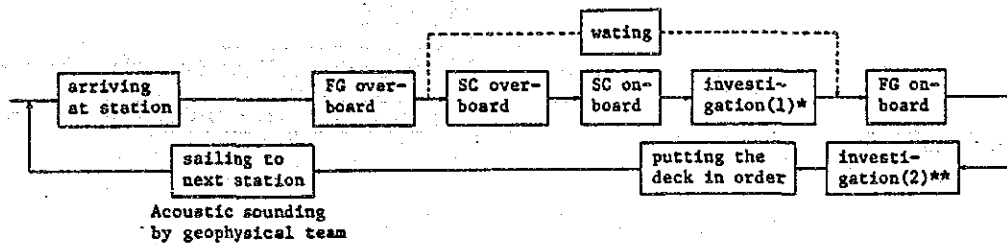
- (1) Possibility of observing the continuity of abundance of manganese nodules around the sampling stations where this abundance was highest;
- (2) The sea area where the embedding ratio of the manganese nodules was low would be suitable for analysis by photos;
- (3) Since the present CDC system does not consist of successive photographs controlled by the towing apparatus kept at a fixed level from the sea bottom, but of intermittent photos controlled by the landing of the shutter sinker, the system was practical even on the violently undulated sea floor and the effect of the sea floor topography might be negligible. Moreover, the results of the secondary survey such as the sampling by FG, observation of the sea bottom by PDR and SBP, geological structure section of the

SUMMARY OF THE EXPLORATION WORK ON BOARD

The exploration work is carried out by the geological team and geophysical team respectively. The main works of the exploration are the bottom sampling and the acoustic sounding.

The outline of the exploration work is as follows:

(A) The outline of the bottom sampling work



* Detail of investigation (1)

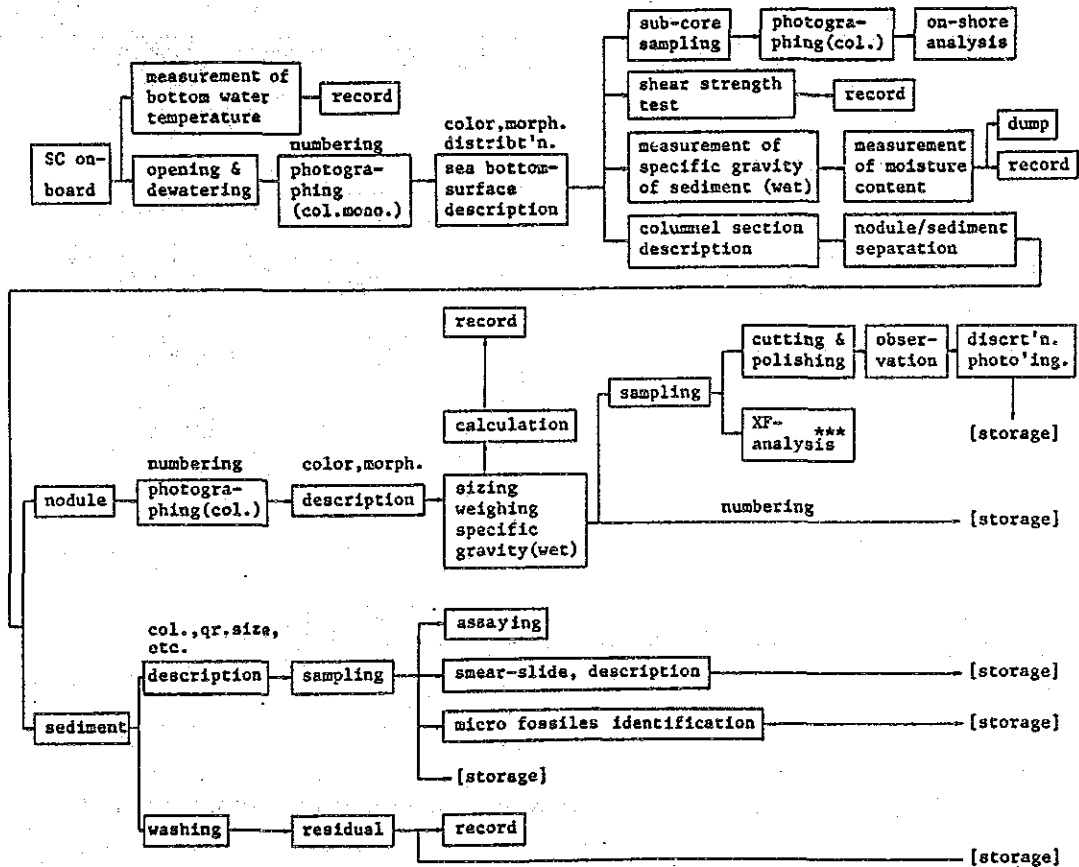
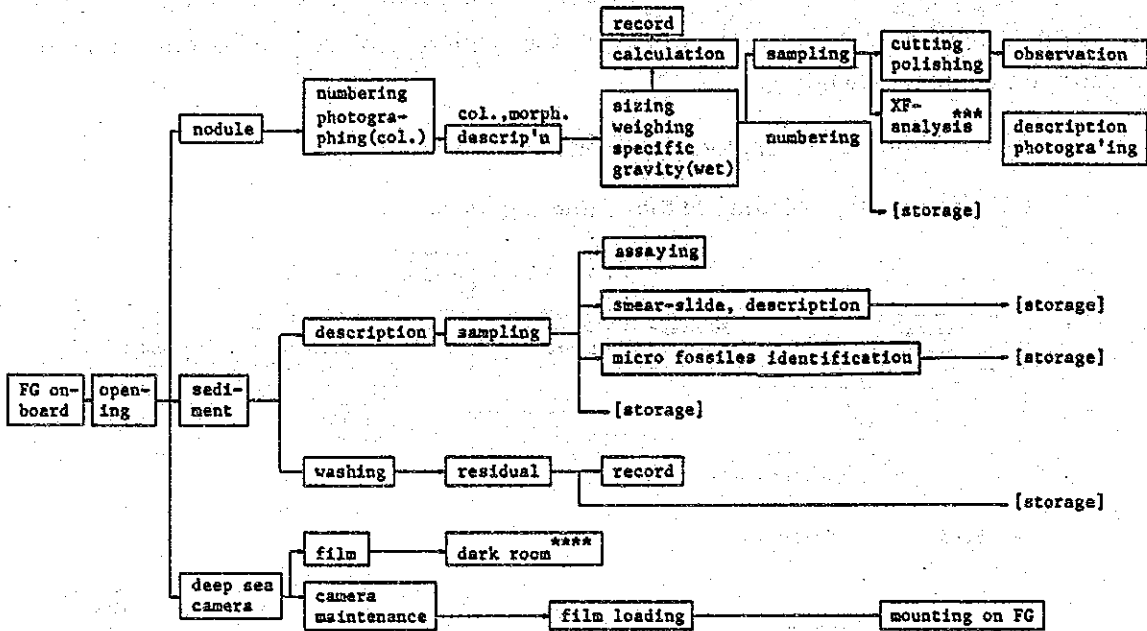
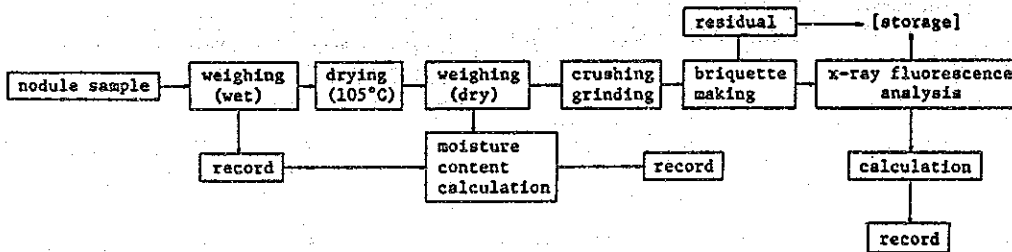


Figure 3-7-1. Processing and Assaying Flowsheet of Samples (No. 1)

** Detail of investigation (2)



*** Detail of XF-analysis



**** Detail of dark room work

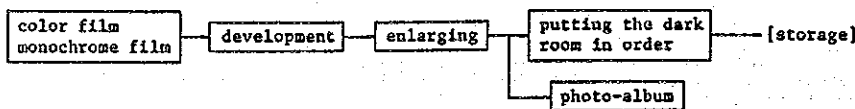
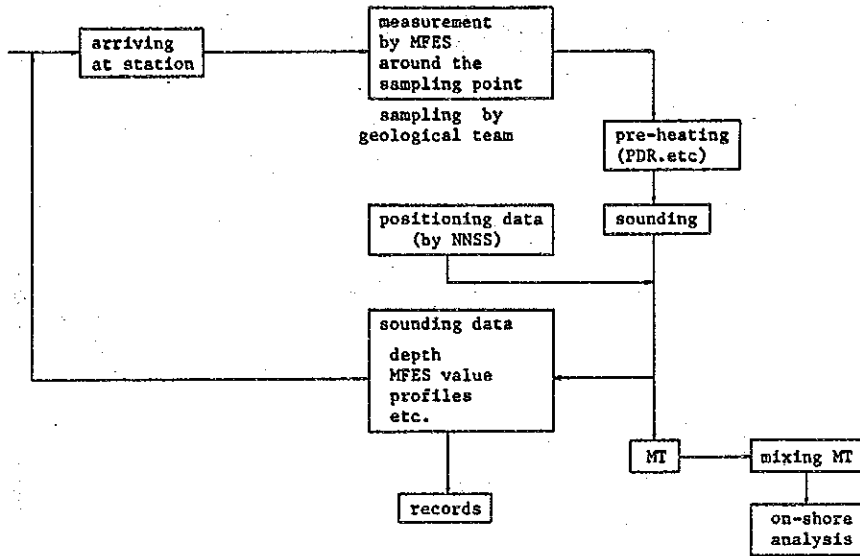


Fig. 3-7-2 Processing and Assaying Flowsheet of Samples (No. 2)

[B] The outline of the acoustic sounding



After surveying, on the way to the base harbor, all data are analyzed and evaluated. The outline of them are as follows:-

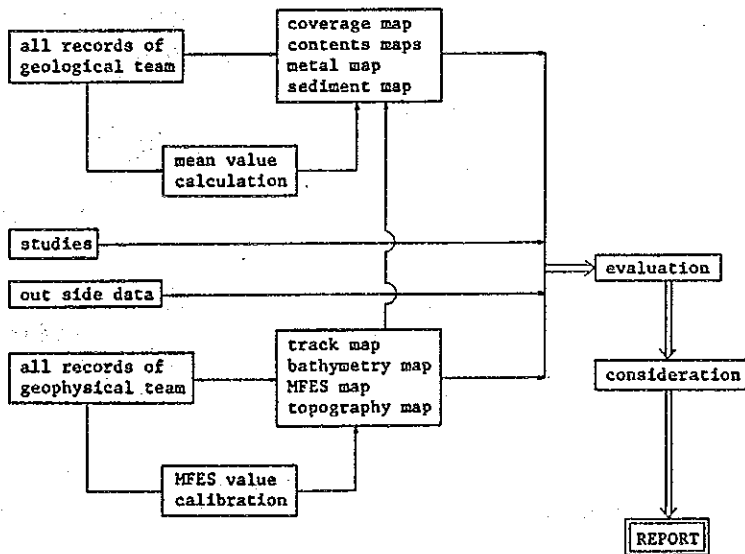
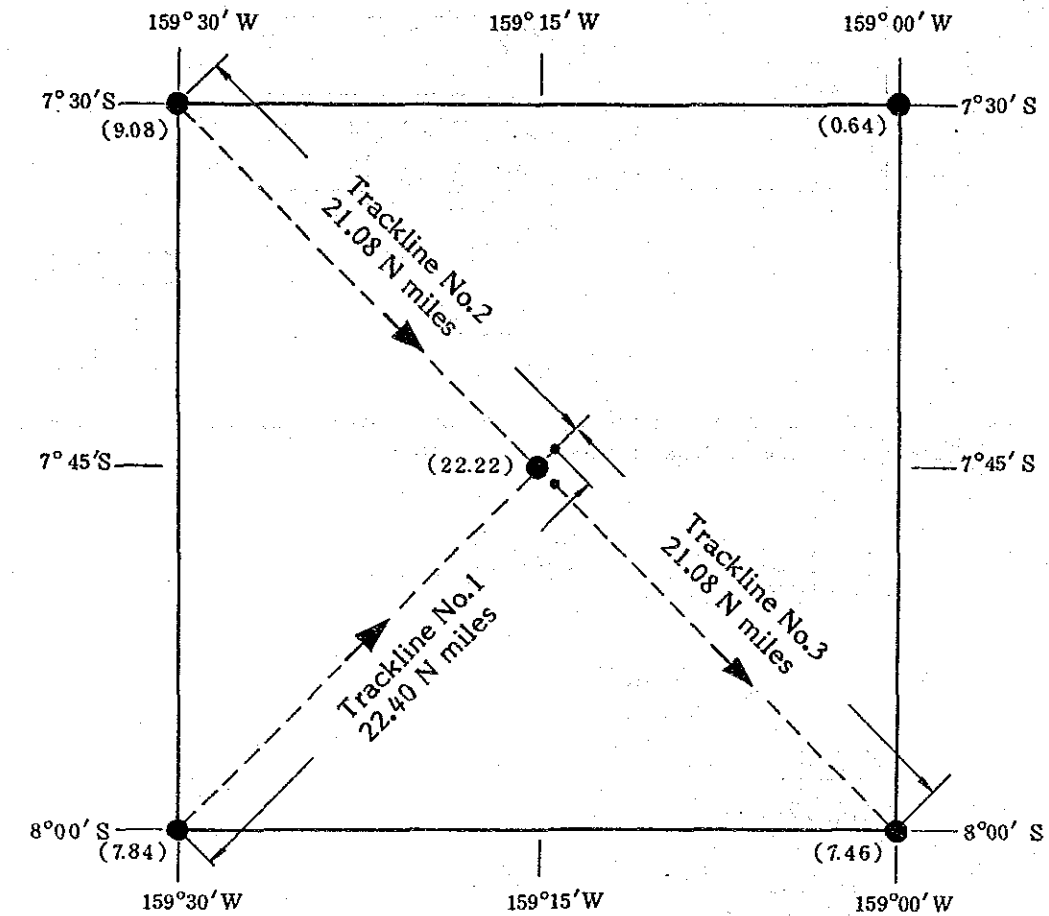


Fig. 3-7-3 Acoustic Sounding and Processing Flowsheet

sea bottom, measurement by MFES, were also taken into consideration as part of the overall examination. Finally, the three track lines with a total length of 64.56 nautical miles were selected, as shown in Fig. 3-8-1.



➔ : Towing direction of CDC

() : Average abundance of the manganese nodules by FG (kg/m^2)

Fig. 3-8-1 Track Lines of Sea Bottom Observation by Means of CDC

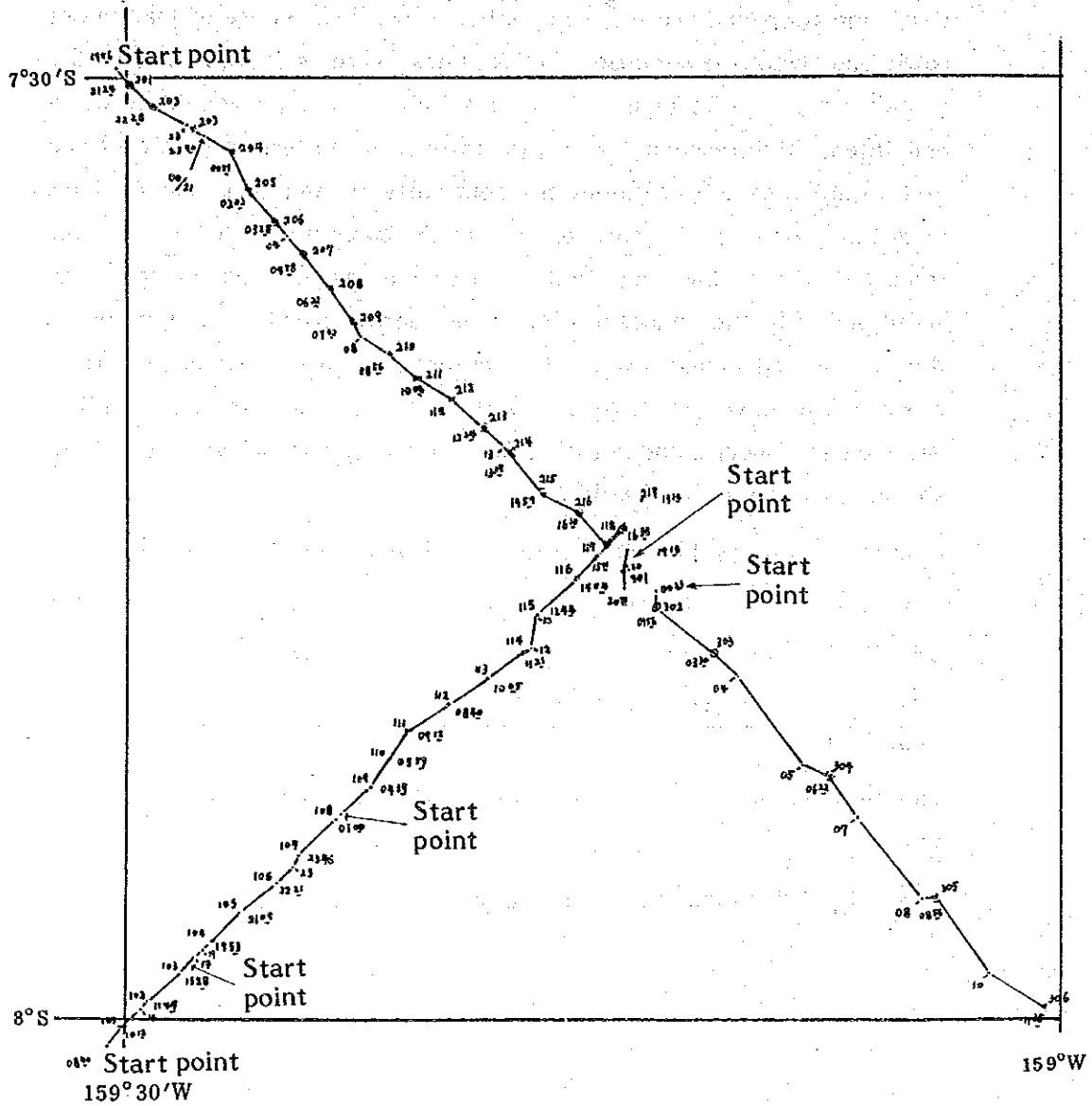
2) Interval of observation stations of CDC

In determining the interval distance between the observation stations of CDC, the following are the principal reasons: In the case of track lines No.1 and No.2; observation track lines were selected where the abundance should be high and the sea floor topography could be quite undulated, the interval between the stations was determined to be fixed at 1.33 miles so as to examine the continuity of the manganese modules in detail. Also in the case of line No.3, observation track line was selected where the sea floor topography is less undulated, and simultaneously the abundance has a decreasing trend in proportion to the distance advanced towards the southeast from the origin, therefore, the interval between the first two stations was fixed at 1.33 N miles, between the second and third at 2.65 N miles, and between the third and the last one at 5.3 N miles.

Line No.	Interval between stations	Number of stations
No.1	1.33 (N miles)	18
No.2	1.32	17
No.3	1.33, 2.65, 5.3	6
Total		41

The total number of the observation stations as above-mentioned is 41.

Also, Fig. 3-8-2 indicates the locality of the observation stations.



Explanatory notes:

101 - 306

Stations' number

01:56 - 23:46

Starting time of photographing

Fig. 3-8-2 CDC Observation stations

3) Number of photos by CDC

The number of photos taken at each station were 5 for the stations where the undulation of sea floor is quite obvious and 4 - 3 for the stations where the undulation is less.

4) Photographing operations of CDC

From 08:00 October 19 when preparations for setting down of CDC were started (at 09:00 CDC was set down) until 13:30 October 22 when re-collecting was over, that is to say, during the time lapse of 77:30, photographing operations at 41 stations, as scheduled in the program were achieved.

Of the 168 photographs taken, 137 were adopted meeting the requirement for analyzing the abundance and the size of manganese nodules; the remaining 31 photos were excluded, because photos pictured only basement rock or because the shutter sinker did not appear to serve as a measuring scale.

The photography operation was carried out on the basis of the sea floor topography section established previously by the PDR operation on the track lines.

5) Analysis of the photos by CDC

As for the analysis of photos, in accordance with the sea bottom photos and the size of shutter releasing sinker pictured in them, the covering surface ratio (COV) of the manganese nodules and their number (N) per 1 m² were determined. Then, using the following regression equations *1, the abundance and average of granular diameter are calculated:

$$\text{Abundance (kg/m}^2\text{)} = 1.430 \times \text{COV}^{1.5}/\text{N}^{0.5}$$

$$\text{Average of diameter (cm)} = 16.62 \times (\text{COV}/\text{N})^{0.5}$$

*1 In relation to the abundance, the covering surface ratio and the number of manganese nodules, the regression equations were established and the coefficient was determined.

These formulas are applied respectively to the 137 photos suitable for photographic analysis.

The average of abundance and the average size at every station are determined by arithmetic mean of the respective values of the analyzed photos taken on the concerned station.

In the case of the photos (11) picturing only basement rock, they were added up to calculate the mean value of each station, assuming that the number of manganese nodules is zero.

3-9 Evaluation of the Grab Operations by FG Sampler and of the Sample collecting Accuracy

The amounts of samples obtained by FG could not be sufficient, it would be assumed that it had happened because of net damage, of teeth breaking or incomplete operations, though it was a rare case. (cf. Fig. 3-9-1)

When these cases were ascertained, the covering surface ratio (a) and re-collecting surface ratio (b), were used to fix the operating accuracy of grabs by dividing the evaluation of the re-collecting accuracy in 4 ranks, the covering surface ratio on the sea bottom photos were compared with the re-collecting surface ratio; and these processes served as reference to calculate the abundance.

3-10 Processing and Analyzing of the Survey Data

The processing and analyzing of the survey data were carried out mainly on board, however, a part of the data processing and synthetic analyzing were executed on shore.

		a (%)				
		0	5	10	20	100
a/b	> 1.00	1	1	1	1	
	1.00	1	1	1	1	
	0.75	1	2	2	2	
	0.50	1	2	3	3	
	0.25	1	2	3	4	
	0.00	1	2	3	4	

- | | |
|----------------------------------|-----------------------------------|
| 1. (Collection) complete | a: Coverage (deep sea camera) |
| 2. (Collection) fairly completed | b: Coverage |
| 3. (Collection) incomplete | (calculated on samples collected) |
| 4. (Collection) failure | |

Fig. 3-9-1 Calculating Criteria of Grab Precision

1) Survey data and its processing

① Relating to cruising and acoustic sounding:

- o The vessel positions by NNSS (data, time, latitude, longitude) were formulated in the table of rectified vessel positions for every minute and were out-put from the data processing system on board.
- o The depth values by PDR (NBS) (data, time, values reported from the digitizer and print out papers) were registered in the field notes every 5 minutes.
- o The superficial sediments by SBP (thickness of upper transparent layers, stratigraphy type) were registered in the field notes every 10 minutes.
- o The measuring values of MFES were registered to the disk of computer every 10 minutes on the track lines between the sampling stations, and every 5 minutes between the sampling points respectively.

② Relating to sampling:

The survey data on manganese nodules, sediments, and assay etc., were processed for every sampling point to be registered in the field notes. The following are the processing taken place on board.

- o Data relating to the manganese nodules: sampling amount, wet weight of each size, wet specific gravity, morphology, No. of superficial structure, etc.
- o Data relating to the sediment: type of sediments, color tone, granular size, microfossil, etc.
- o Data relating to analysis: grade and water content of 5 principal components (Ni, Cu, Co, Mg, Fe)

③ Various photos:

- o Sea bottom photos by deep-sea camera equipped on FC and SC, and by CDC, re-collecting photos, working photos, and etc.,
- o Record photos of physical prospection (PDR records, SBP records)

2) Analyzing of the survey data

Every necessary figures which was essential for advancing the survey, were drawn up on board using the data up-dated, and later these data were reanalyzed on shore in detail more. The following are the outline of products described in the following:

① Chart of track lines, location map of sampling points

Chart of track lines was drawn up first, using the table of rectified vessel positions printed out from the data processing system and then location map of sampling points plotting the position on a 1/1,200,000 scale registering sheet (published by the Hydrographic Division).

② Map of the sea floor topography

Using the sea depth chart, that is to say, the above-mentioned track lines chart plotted with depth values every 10 minutes, the map of sea floor topography was drawn up depth contours with the 200 m interval.

③ Thickness contour map of the upper transparent layers by SBP

Thickness of the upper transparent layers' was read out every 10 minutes from the SBP record and plotted on the above-mentioned chart of track lines. Then the contour map with 10 m thickness was completed. (auxiliary contour lines of 5 m thickness were added for the part with 0 - 10 m thickness.)

④ Distribution map of bottom materials

Distribution map of bottom materials was completed by superimposing types of bottom materials taken by means of mud collector on positions of sampling points and by plotting the quantity and names of authigenic minerals obtained with manganese nodules by means of F.G.

⑤ Abundance of manganese nodules estimated by MFES

Abundance of manganese nodules estimated by MFES was accomplished by plotting the abundance (MFES intensity) displayed every 10 minutes. Abundance contour lines was drawn up with the step of 2.5 kg/cm^2 .

⑥ Abundance map of manganese nodules, grade contour map, metal quantity map

On the basis of data obtained on the manganese nodules at each sampling point (setting down point of FG, SC, etc.), the average occurrence situation of minerals (values of abundance and grade etc.) was determined for each station (3 samplings per one station), and the following are the products by processing these determined results: the figure of the abundance of manganese nodules; the figures of the grade contour of nickel, copper, cobalt, manganese and iron; and the figure of the metal quantity of nickel, copper, and cobalt. In addition, the acoustic sounding data were utilised in this process.

⑦ List of the survey results

In order to facilitate searching and consulting of the data on the manganese nodules obtained every day on board, the essential items *1 were listed up from the field notes and the survey results were arranged in the list.

*1 The principal itmes are as follows:

latitude, longitude, sea depth, granular size distribution, values of abundance, morphology, grade, sediment, state of combinations, etc.,

⑧ Estimated abundance by CDC observation

Estimated abundance map by CDC observation was accomplished by plotting sampling data concerned and these calculated from coverage of manganese nodules on the CDC photos using the regression formula introduced by analyzing FG sampling data statistically.

⑨ Other

Observing the relation between each of the elements such as the bearing quantity of the manganese nodules, grade, morphology, bearing situation, topography, upper transparent layers' thickness, etc., studies have been carried out to define the potential field of manganese nodules.

Chapter 4. Results of the Survey

4-1 Survey accomplishments

The surveying operations were accomplished as shown in Table 4-4-1.

Table 4-1-1 List of the survey accomplishment

	Item	Accomplishment
Survey schedule	Leaving the port of Honolulu Arrival the survey areas Leaving the survey areas Entry to the port of Honolulu	Sept. 24 16:00 (*) Sept. 30 06:00 (*) Oct. 22 13:20 (*) Oct. 28 08:00 (*)
Sampling	Accuracy (disposition of the stations) Sampling stations Sampling per one station Samplers used Failure due to non-floating	Stations at the primary stage (42.4 N miles grid) and Stations at the secondary stage (21.2 N miles grid) 38 points 3 samples Free fall samplers (110 samplings) Spade corers (4 samplings) None
Deep-sea camera	Use of deep-sea camera - successful cases - unsuccessful cases due to	114 times of which 99 times 15 times - disorder in batteries 4 times - premature flash 8 times - malfunction of shutter 3 times
Photo analyzing	Photo analyzing - analyzing of FG, SC photos - analyzing of CDC photos	267 cases of which 99 cases 168 cases

(continue)

(*): In local time at the 150° W

(Continue from previous page)

	Item	Accomplishment			
Assaying	Treatment	190 cases			
	Analyzed components Total No. of analyzed components	Ordinary samples 187 cases extra ordinary samples 3 cases 5 components; Ni, Cu, Co, Mn, Fe 190 cases x 5 components = 950 components			
Acoustic sounding	SBP 3.5 kHz	Distance of sounding surveyed: 2,659 N miles			
	PPR 12.0 kHz	"			
	NBS 30.0 kHz	"			
	MFES	"			
Data processing	On line MT	6 reels			
	On line MIX MT	5			
	Sampling MT	2			
	Sampling MIX MT	1			
	Atmospheric and marine meteorogy MT	2			
	Atmospheric and marine meteorogy MIX MT	1			
	(Total)	(17 reels)			
Sea bottom observation by CDC	Name of track lines	85SCDC01	85SCDC02	85SCDC03	Total (average)
	Total length of track lines (mile) (A)	22.40	21.08	21.08	64.56 miles
	No. of surveyed stations	18	17	6	41
	Required hours	31:02	23:09	17:19	71:30
	setting hours	04:26 *	01:28 **	03:05 ***	08:59
	moving (T)	08:19	07:45	06:12	22:16
	preparation	09:00	09:20	03:38	21:58
	photographing	05:00	03:14	00:53	09:07
	re-collecting	04:17 *	01:22 **	03:31 ***	09:10
	average speed (A/T) (knot)	2.69	2.72	3.19	(2.84)
	average minutes of photographing (min./pcs)	3.37	2.62	2.41	(2.96)
No. of photos ****	81/(90)	69/(74)	18/(22)	168/(185)	

*: for 3 times,
 **: for once,
 ***: for 2 times
 ****: No. of successful photos/No. of photos

4-2 Sea Floor Topography

1) Classification of sea floor topography

To analyze the bearing situation of manganese nodules, the topography was classified from regional and local points of view.

Table 4-2-1 Classification of Sea Floor Topography

Topographical classification		Definition
Regional province	Plain	Area whose bottom is almost flat and even with a isolated sea mount or sea knoll, it may be considered as plain from a general point of view;
	Hilly	Area where numerous sea hills or sea mounts are dispersed;
	Mountainous	Area where a group of sea mounts are located;
	Quasi- plain	Area where the outstanding mounts or hills are scarcely observed but the bottom is rather undulated and which is classified neither as plain nor as hilly.
Local area	Flat	Plain area not undulated or smoothly undulated (up to about 100 m relative height) and which doesn't belong to neither the hollow nor the platform.
	Hollow	Area with smooth undulation and which presents a generally concave terrain, including a ship- shaped basin.
	Channel	Long and narrow concave terrain in a ditch shape, including fissures or fracture zones.
	Platform	Area with smooth undulation which presents as a whole a convex terrain (or a tableland)
	Sea Knoll	Hilly area with a relative height of more than about 1,000 m, including entire slop as well as summit
	Sea mount	Hilly area with a relative height of less than about 1,000 m, including entire slop as well as summit (the sloping surface contains a shifting part of the plain)
	Ridge	Terrain presenting a chain of mountain composed of the sea knolls and hills ranged in a zone.
Other	Terrain not belonging to any of the above-mentioned classifications.	

The sea floor topography of the surveyed areas belongs to the plain province macroscopically and is classified into 5 types microscopically such as plain, hollow, platform, sea knoll and sea mount.

2) Characteristics of the sea floor topography

The present surveyed areas are located at the western edge of the northern Penhryn basin, eastern margin of the vast Manihiki plateau (relative height of 1,500 - 2,000 m) and to the North of Penrhyn Island.

The depth of the surveyed areas is generally between 5,300 - 5,500 m, except for the sea mounts and sea knolls, as shown in the Fig 4-2-1 and Fig. 4-2-2 explaining the sea floor topography and in the Figure of the sea floor topography (cf. Annexed figure 3).

As for the general characteristics of the surveyed areas, it appears that the hilly forming the outside margin of the Manihiki plateau, the western edge of areas (west of 159° W), present a complex and intensely undulated topography. The sea mounts and knolls range in the east-west direction at the middle (on the 7° 30'S line) of surveyed areas.

3) Local topography around sampling points

The flats are widely distributed in the middle and eastern part of the surveyed areas.

The hollows (including the ship-shaped basins) are dispersed in the western part (around 159° W), but their directional trend was not particularly observed.

As for the platforms, there are no outstanding cases; however, in the western part (around 159° W) a few platforms are scattered.

The sea knolls are distributed in the western part of the surveyed areas and constitute the outside margin of the previously mentioned Manihiki plateau. Their relative height is approximately 650 - 700 m.

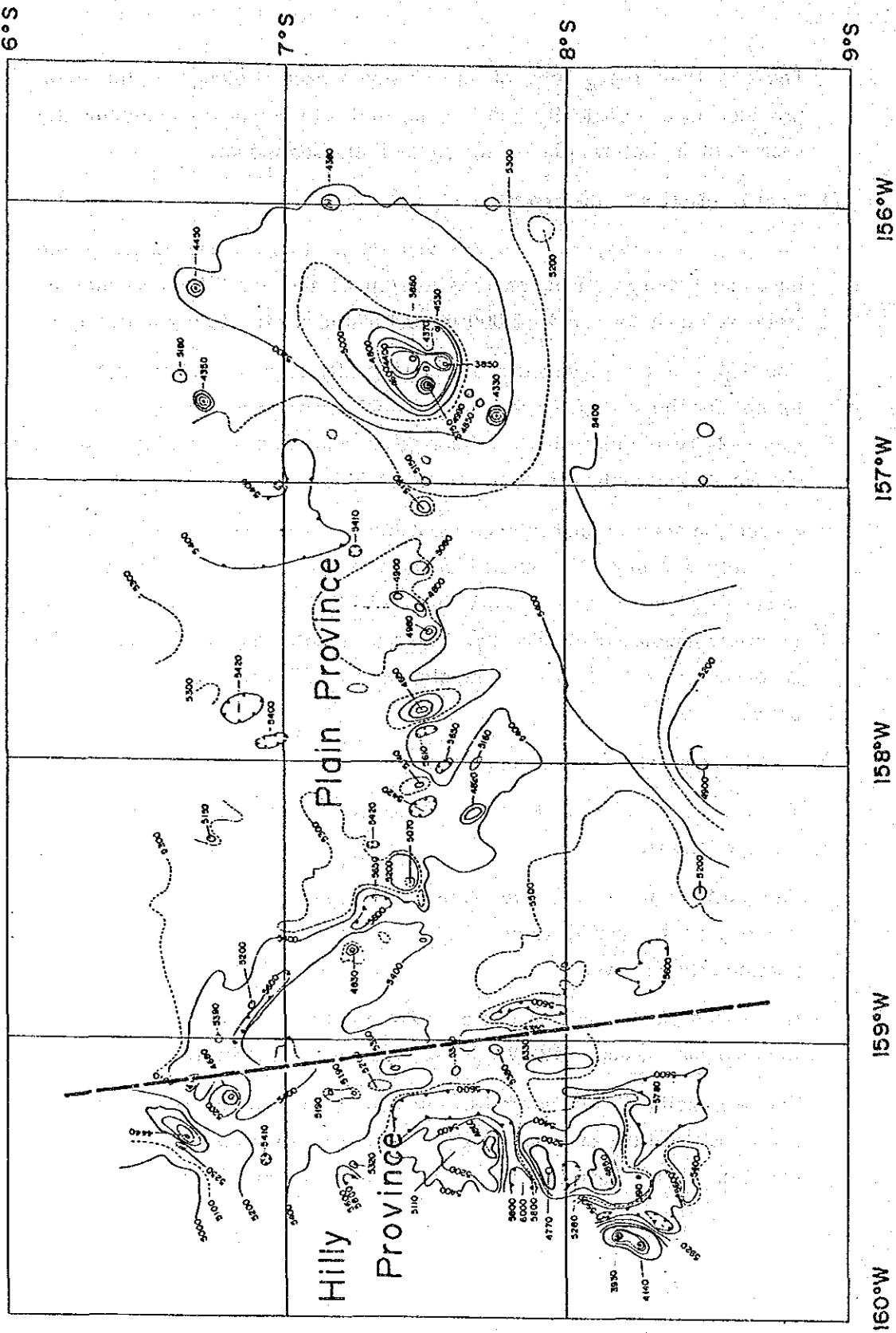


Fig. 4-2-1 Explanation on Sea Floor Topography

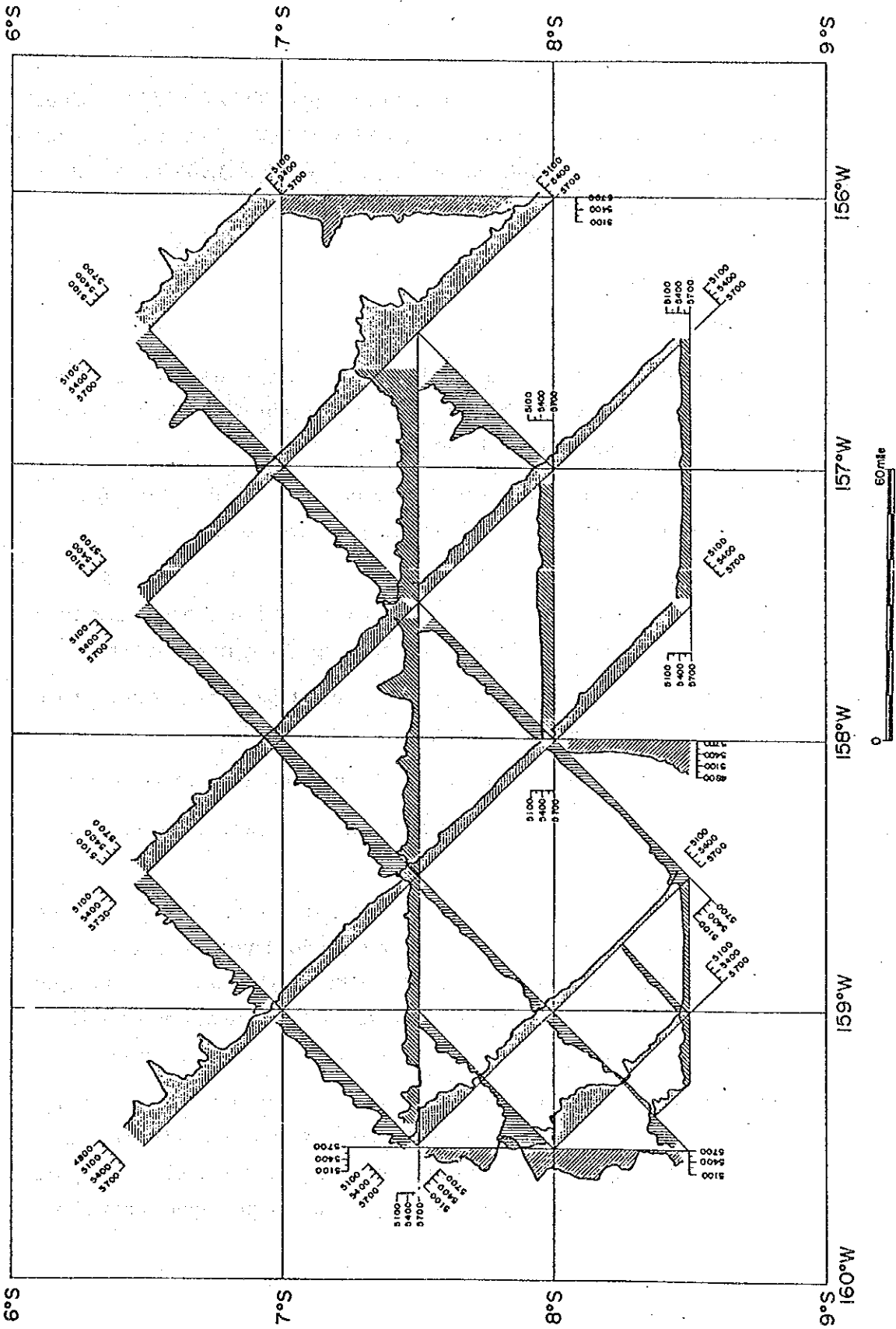


Fig. 4-2-2 Section of the Sea Floor Topography

The sea mounts stand around the southwest part ($8^{\circ} 15'S$: $159^{\circ} 45'W$) of the surveyed areas and in the east part ($7^{\circ} 30'S$: $156^{\circ} 40' W$); at their summits, the water depth measures about 3,700 - 3,900 m and their relative heights are approximately 1,400 - 1,700 m.

4-3 Superficial Sediment

1) Classification of SBP records

Owing to past experience in surveying activities, MMAJ has classified the SBP records, on the basis of their reflection patterns, in 8 types such as type a, b, c, d1, d2, d3, e1 and ts.

In the surveyed areas, among the above-mentioned SBP records, 6 types were observed, but types a and ts were not recognized.

Further, as the type of SBP records obtained in the surveyed areas presented a new reflection pattern which had not been classified before, this was classified separately as a type to be newly set up.

According to the reflection patterns, this type has a intermediate characteristic between types b and c.

The classifications, their definition and characteristics are as follows:

- (1) Type for which the acoustically transparent layers are recognized at their upper part. (cf. Fig. 4.3-1)

Type a: presenting a double layer structure of transparent and opaque, the transparency of the transparent layer is high (faded out completely) and the boundary with the opaque layer is relatively clear; the thickness of the transparent layer measures 10 - 50 m; however, this type was not recognized in the surveyed areas.

Type b: similar to type a, composed of two layers such as semi-transparent and opaque, but the transparency of the semi-transparent layer is not so high as to be called complete transparent; also the boundary with the opaque layer is not clear.

The thickness of transparent layers measures 30 - 100 m and generally speaking it is not a rare case that the thickness could be more than 50 m; the thickness varies markedly as compared with other types.

Type e1: presenting the multistratified structure of transparent and opaque layers; the clearly stripped and thin opaque layer is recognized directly under the upper transparent layer. The layer thickness of this type is generally 10 - 40 m including this stripped opaque layer.

- (2) Type for which the acoustically transparent layers are not recognized at their upper part. (cf. Fig. 4-3-2)

Type c: the type composed of 3 layers: opaque, transparent and opaque; though it was not confirmed on the print-out papers, it is presumed that an external thin transparent layer could coexist at the top of the upper transparent layers.

Type d1: Composed only of opaque layers. Generally, this type is found at the sea mounts, sea knolls, etc., and these sites correspond approximately to their exposed basement rocks.

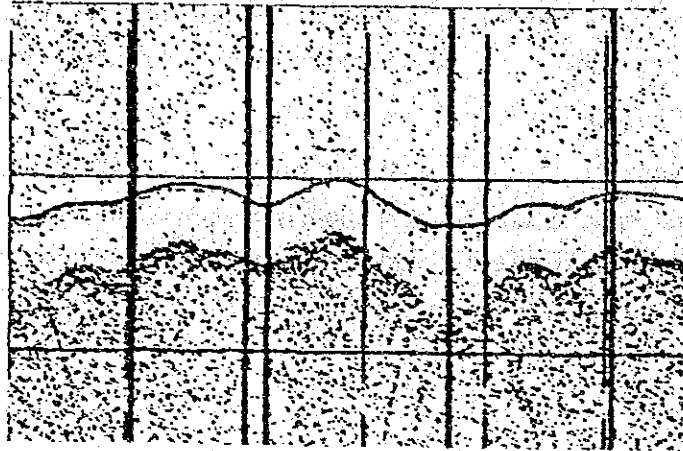
Type d2: similar to type d1, it is composed only of the opaque layers; this type is observed at plains.

- (3) Other (cf. Fig. 4-3-3)

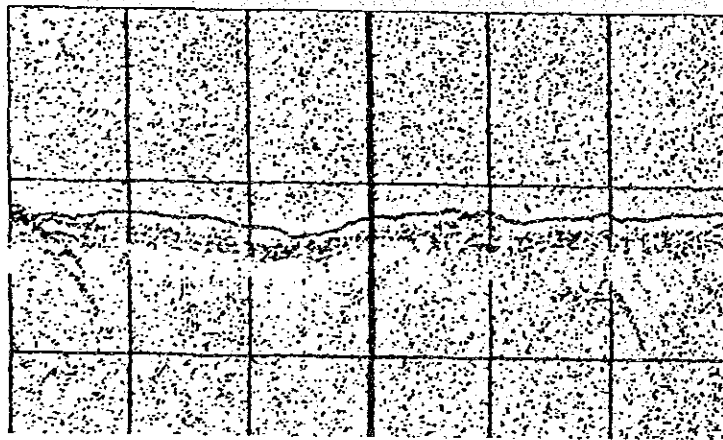
Type ts: it may be presumably composed of transparent and opaque layers; for this type, the records are not clear because of the dispersion of sounding waves by the uneven floor.

Type ds: it may be presumably composed of opaque layers; in the same way as type ts, the records are not clear because of the dispersion of sounding waves by the undulated floor.

Type bc: basically, it may be composed of 2 layers: transparent and opaque, similar to type b; the bottom surface of the top

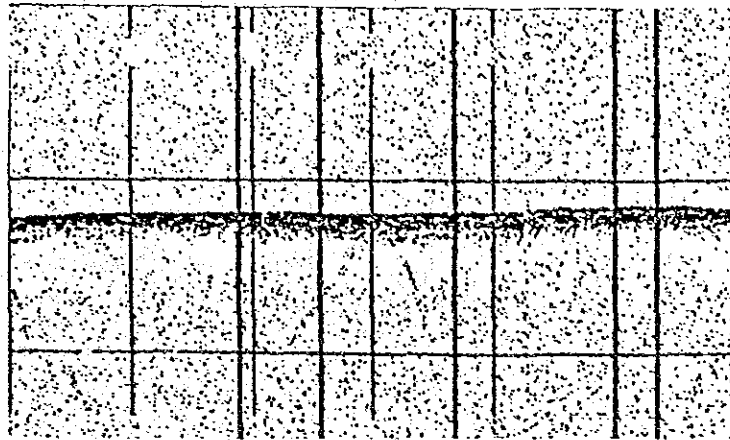


Type b ($6^{\circ}30'S, 158^{\circ}30'W$)

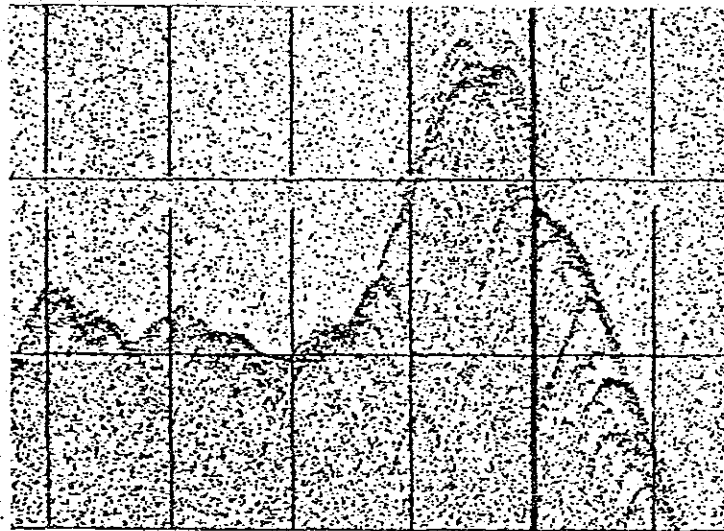


Type e₁ ($7^{\circ}35'S, 159^{\circ}15'W$)

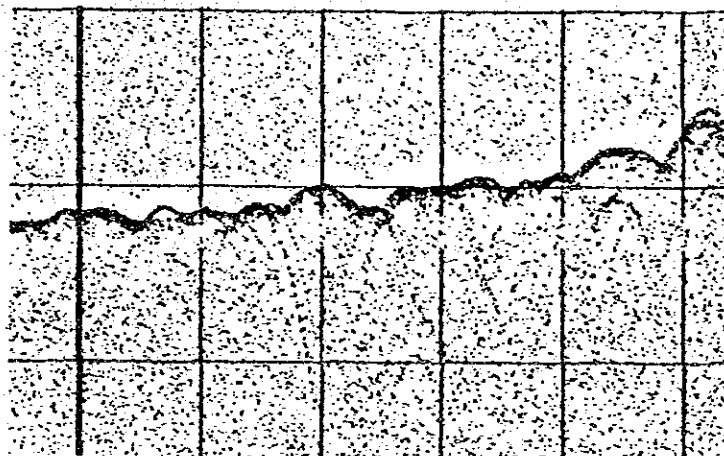
Fig. 4-3-1 Classification of SBP Records (No. 1)



Type c ($8^{\circ}15'S, 158^{\circ}00'W$)

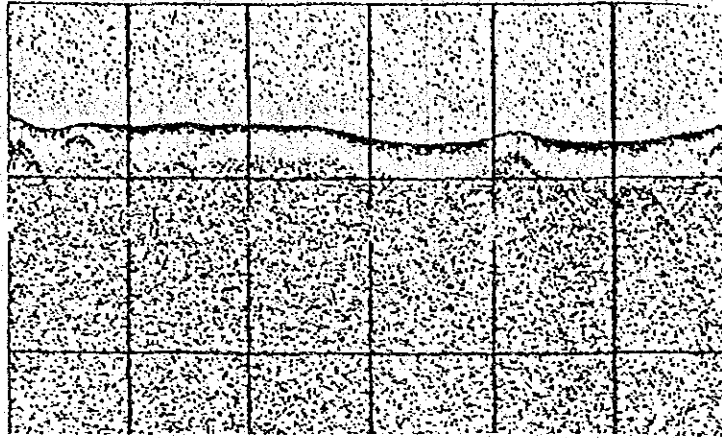


Type d₁ ($7^{\circ}33'S, 157^{\circ}33'W$)

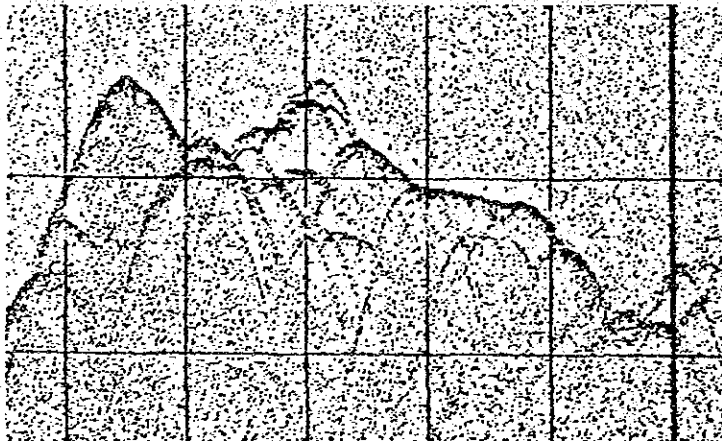


Type d₂ ($8^{\circ}15'S, 158^{\circ}00'W$)

Fig. 4-3-2 Classification of SBP Recorders (No. 2)



Type bc ($7^{\circ}08'S, 158^{\circ}53'W$)



Type ds ($7^{\circ}44'S, 157^{\circ}44'W$)

Fig. 4-3-3 Classification of SBP Recorders (No. 3)

superficial layer indicating a transparent layer does not form one line but contains some noise and presents the opacity. It could be considered as type c whose top superficial layer is thin. The transparency of transparent layers is high.

2) Distribution of SBP types (cf. Fig. 4-3-4)

From the view point of sea floor topography, the surveyed areas are classified roughly with the hill region (called the western region) corresponding to the external margin of Manihiki plateau and the plain region (called the eastern region) occupying the greater part of the surveyed areas *1. The distribution pattern of SBP types has a directional trend; in the western region north-south and in the eastern region east-west.

The distribution of SBP types is also distributed macroscopically in accord with the classification of the sea floor topography and with the depth distribution. From a rough point of view, the type e1 is found in the vicinity of 7°30'S line in the central part of the eastern region *2, the type bc is widely distributed in the northern side of the eastern region.

(1) Eastern region

① North side of the eastern region

In the north side of the surveyed areas the water depth become shallower than 5,400 m. Type b is distributed to a wide extent in this shallower part, especially to the north of 7° 15'S and to the east of 156° 50'W.

*1 The surveyed areas, in general, are separated into an eastern region and a western region by the longitudinal line 159° W.

*2 According to SBP types, the eastern region could be divided, into 3 parts: i.e. north side, central part and south side of the eastern region from north to south.

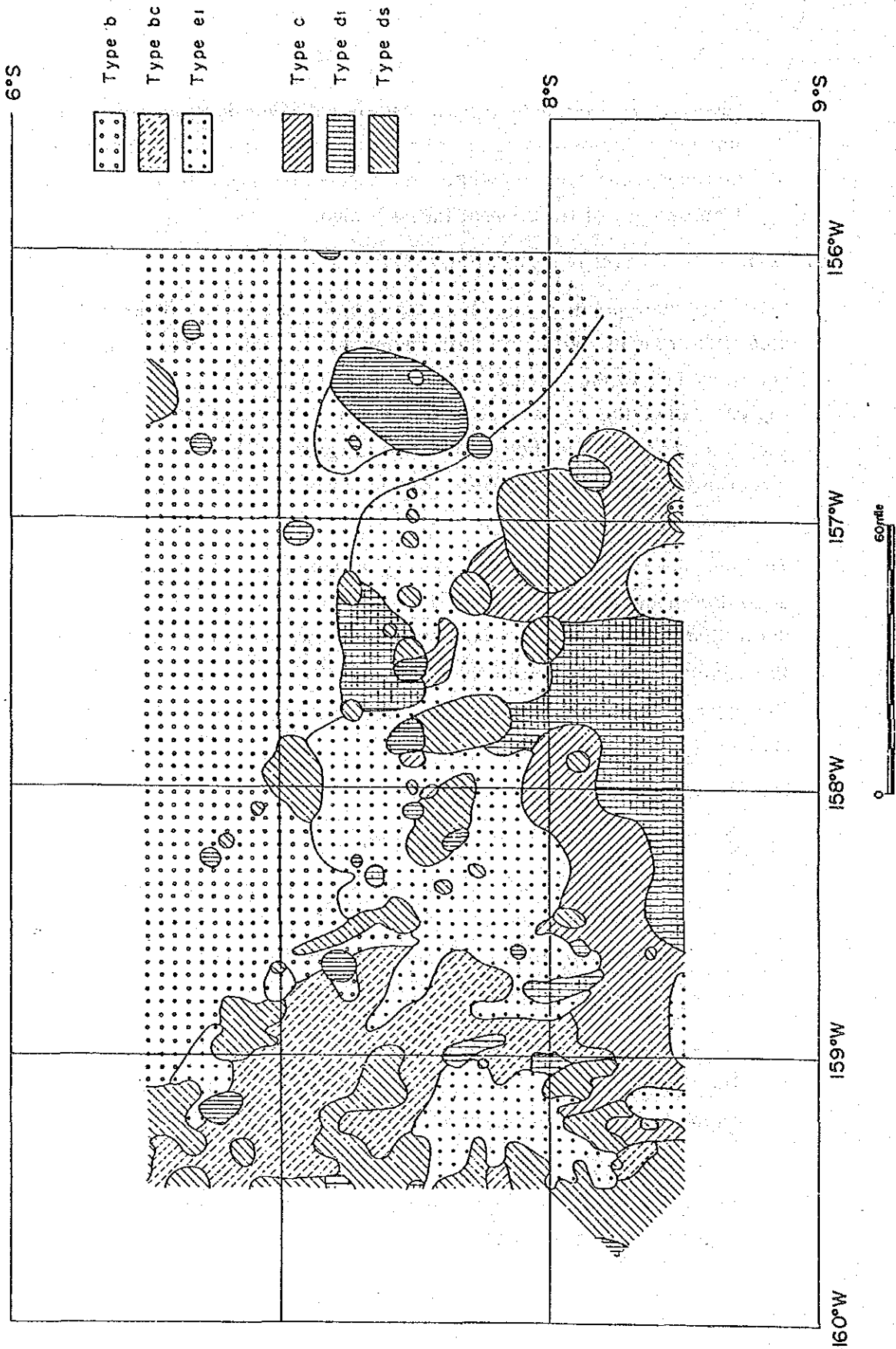


Fig. 4-3-4 Distribution of SBP types

Typical ones of type b are observed around the north side. The thickness of type b is most marked around the west of this north side and becomes thinner towards the central part and east of the north side; the thinnest part measures less than 10 m.

In the middle of the area where the upper transparent layers' thickness is less than 10 m, there exist sea mounts with the type d1; and at the foot of the sea mounts the type b. The depth measures approximately 5,300 - 5,200 m in these areas.

② Central part of the eastern region

At the central part of the eastern region the depth is about 5,400 m, and shows trend of getting shallower towards the north side and deeper towards the west side. The depth contours of 5,400 m are curved complexly because of the dispersed sea knolls and concave terrain.

Distribution of SBP type is characterized according to the respective sea floor topography; type d1 and d2 are dispersed among the sea knolls and elevated terrain; type c appears at the concave terrain and type e1 at the greater part of the floor where the depth measures about 5,400 m.

③ South side of the eastern region

On the south side of the eastern region, the SBP types consist mainly of type e and d2.

Type c is distributed around the concave terrain enclosed by the depth contour of 5,600 m and from this contour to an extent to where the depth measures 5,400 m.

Type d2 is distributed toward the north and on the elevated terrain whose depth is 4,900 m and which is presumably the foot of Penrhyn Island.

(2) Western region

At the western region, in accord with the hill forming an external margin of Manihiki plateau, type d1 and d2 are distributed; in front of this part, type e1 and bc are distributed.

As for type e1, it presents the typical records patterns distributed at the concave terrain of 5,600 m depth; according as the depth becomes shallower, this part is contiguous to opaque layers of type ds etc.; however, a boundary between these two parts is complicatedly curved being influenced by their topography.

Type c is distributed at the part corresponding to the foot of a front margin of the hill. As for type c found at this part, its records pattern is more or less blurred; the survey data could not make it clear whether this phenomena was attributed to exact seizure of superficial sediment on the sea bottom or to reflection of the sea bottom minutely rugged.

3) Thickness and its distribution situation of upper transparent layer in SBP Profiles

The upper transparent layers thickness by SBP and its distribution situation are shown in the annexed Figure 4. This Figure shows that distribution of the upper transparent layers thickness corresponds nearly to that of the SBP type.

Observing the upper transparent layers thickness by respective SBP type, for type b, thickness measures 5 - 70 m; for type bc, 5 - 30 m and type e1, 5 - 10 m (partially 20 - 30 m); while for types c, d1, d2, ds, etc., transparent layer was not recognized.

As for the distribution of the upper transparent layers thickness, what should be mentioned particularly is that except types b and bc, the transparent layers thickness is extremely thin as 5 - 10 m at almost all parts of the surveyed areas.

4-4 Research on Manganese Nodules by Means of MFES

1) Factors affecting MFES

(1) Size of manganese nodules (Weight factor)

By means of MFES, three different frequencies were subsequently measured; NBS (30 kHz), PDR (12 kHz) and SBP (3.5 kHz); and supposing that between the compound sound pressure and the abundance of manganese nodules V (kg/m^2) there exists a linear relation formulated by :

$$V = a \cdot R_t + b,$$

the parameters a and b are defined and the data analysis is practiced.

According to the supposition by means of MFES, the abundance of manganese nodules is proportional to a covering ratio of bottom surface, without any relation with granular diameter in case where their granular diameter remains within 1 - 15 cm.

Therefore, weight per unit covering surface of the manganese nodules was measured independently of MFES.

The average weight coefficient ^{*1} of manganese nodules used for parameter analysis was $2.2 \text{ g}/\text{cm}^2$.

This means that the measured value by MFES is in proportion to the abundance when the measurement is done on the sea area where its weight factor of manganese nodules is $2.2 \text{ g}/\text{cm}^2$.

The weight factor distribution of this sea area is shown in Fig. 4-4-1, and the values are less than $2.2 \text{ g}/\text{cm}^2$ on almost all stations. The weight coefficient of the whole sea area is about $1.6 \text{ g}/\text{cm}^2$.

*1 Weight coefficient = Recovered weight of manganese nodules / (coverage of manganese nodules x grab opening area).

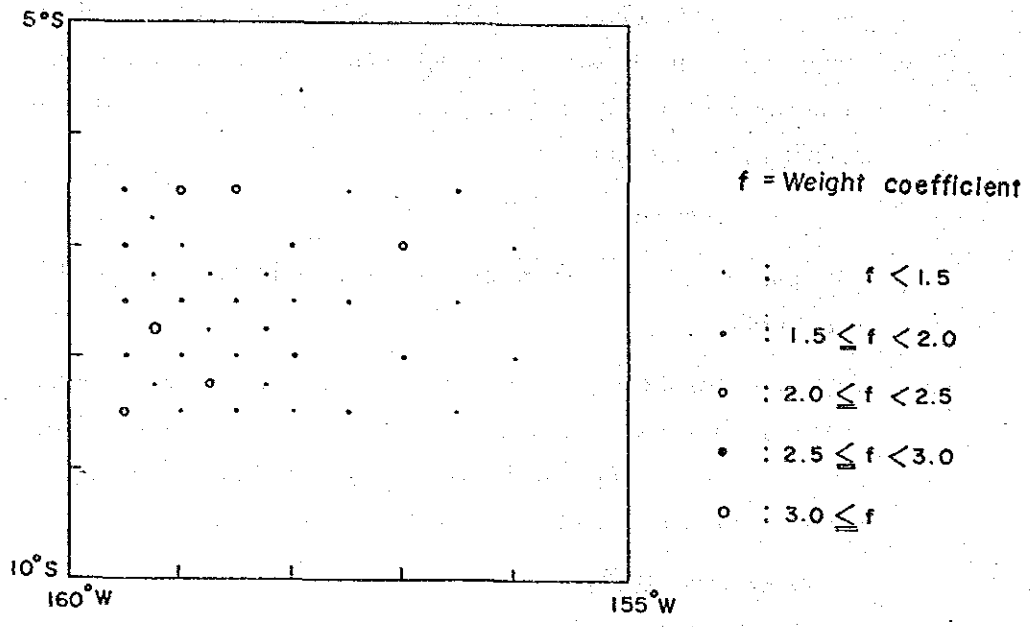


Fig. 4-4-1 Distribution of Weight Coefficient

This indicates that the granular size of manganese nodules in the surveyed areas is smaller than that in the inspected sea area. In other expression, the results obtained by MFES were overvalued in comparison to real values. Therefore, the estimated abundance by means of MFES was re-calculated by the following formula with corrected weight coefficient:

$$\text{Abundance by MFES} = \text{Measured value} \times \text{Weight factor} / 2.2 \text{ (g/cm}^2\text{)}$$

(2) Embedded manganese nodules

As shown in Fig. 4-4-2, the embedded manganese nodules exist predominantly in the surveyed areas, particularly in the palin.

We examined whether the embedded manganese nodules were sufficiently detected by MFES in the surveyed areas.

In case the coverage by samples obtained is greater than the coverage by deep-sea camera, the manganese nodules maybe defined as embedded; in the present report the degree of manganese nodules embedded is considered high in such case as;

$$1 - (\text{coverage by deep-sea camera} / \text{coverage by samples obtained}) > 0.4$$

Theoretically the coverage measured by MFES should be greater than the coverage by deep-sea camera and be equal to the coverage by samples obtained.

These relationships are shown in Fig. 4-4-3.

Comparison between Fig. 4-4-3 (a) and (b) indicates that the coverage measured by MFES is greater than that by deep-sea camera where embedded manganese nodules are predominant. Furthermore, where exposed manganese nodules predominant, the coverage measured by MFES seems to be as great as that of embedded manganese nodules in spite of a small amount of data as shown in Fig. 4-4-3 (a).

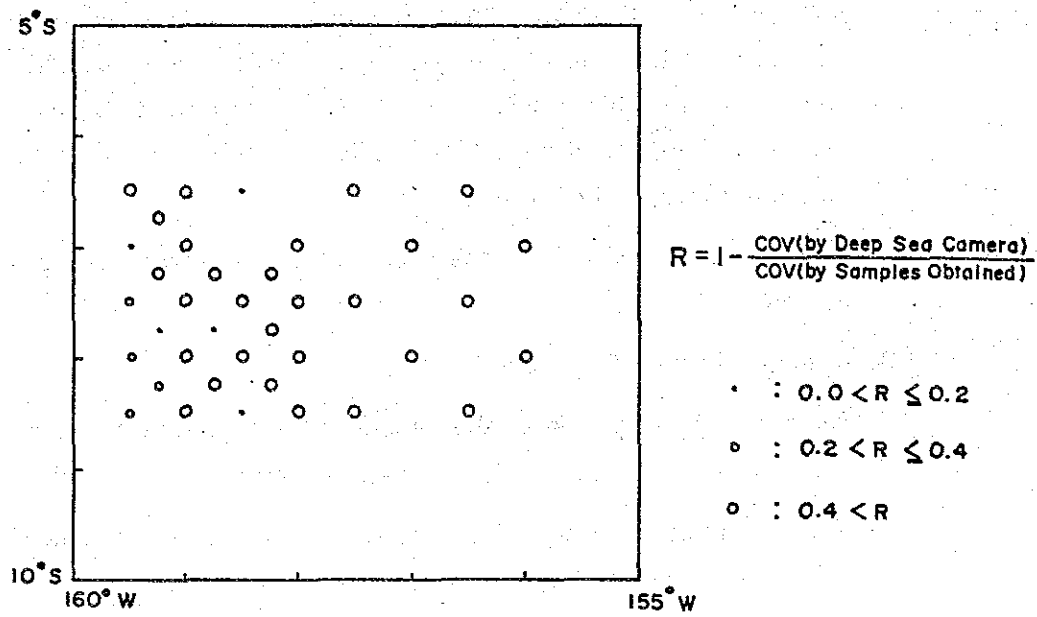


Fig. 4-4-2 Distribution of Embedded Type Manganese Nodules

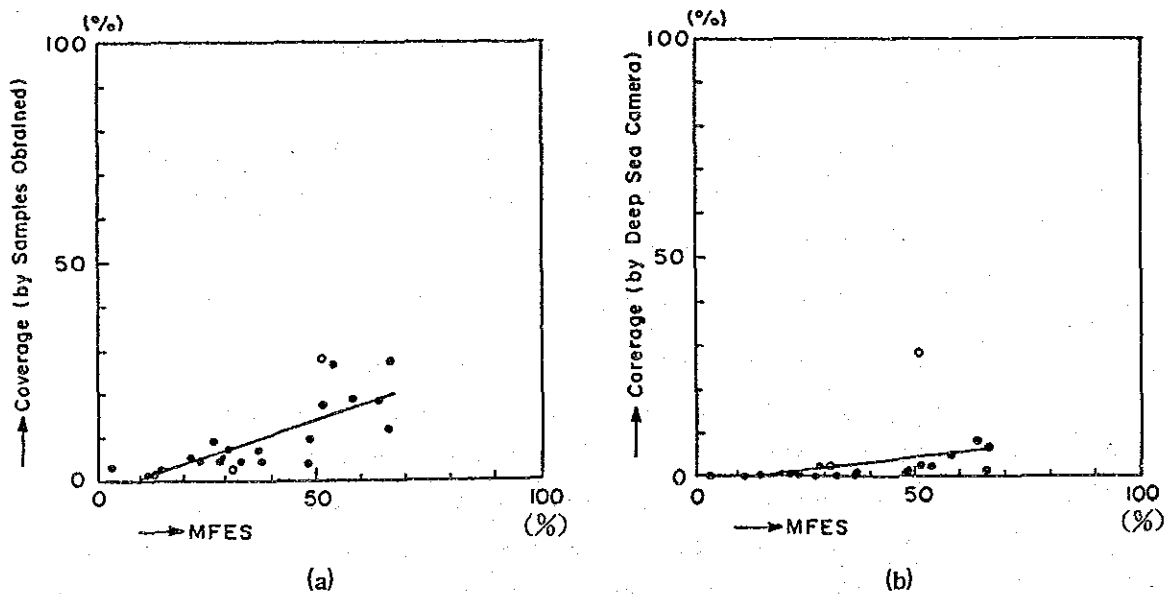


Fig. 4-4-3 Influence of Embedded Type Manganese Nodules on MFES Measurement

Therefore, it may be explained that embedded manganese nodules were well detected by MFES in the surveyed areas.

(3) Topography and bottom materials

As shown in Fig. 4-4-4, the correlation coefficient between the MFES intensity and the abundance of manganese nodules indicates more than 0.7. This is in relatively good correlation but is not enough and is rather dispersed.

As described in the paragraph on the sea bottom topography, we paid attention to the fact that the sea bottom topography in the surveyed areas is divided into two zones; one in the western hills, another in the eastern plains, with its border on the 159°W line.

Therefore, we prepared statistics separately with selected sample data for both zones. (cf. Fig. 4-4-5)

The results are shown in Fig. 4-4-6.

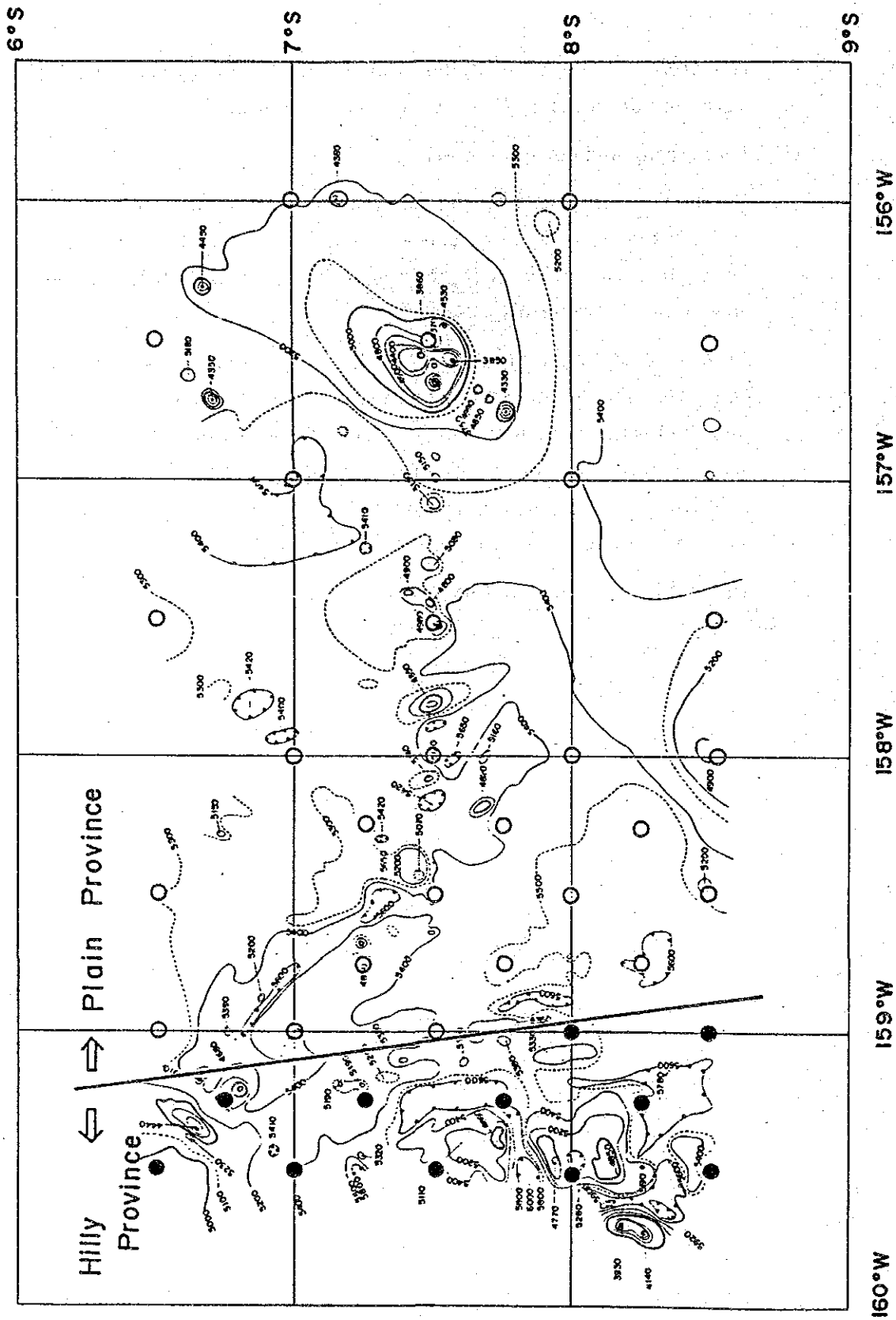


Fig. 4-4-4 Classification of Sampling Stations into Plain and Hilly Provinces ● Sampling Stations in Hilly Province ○ Sampling Stations in Plain Province

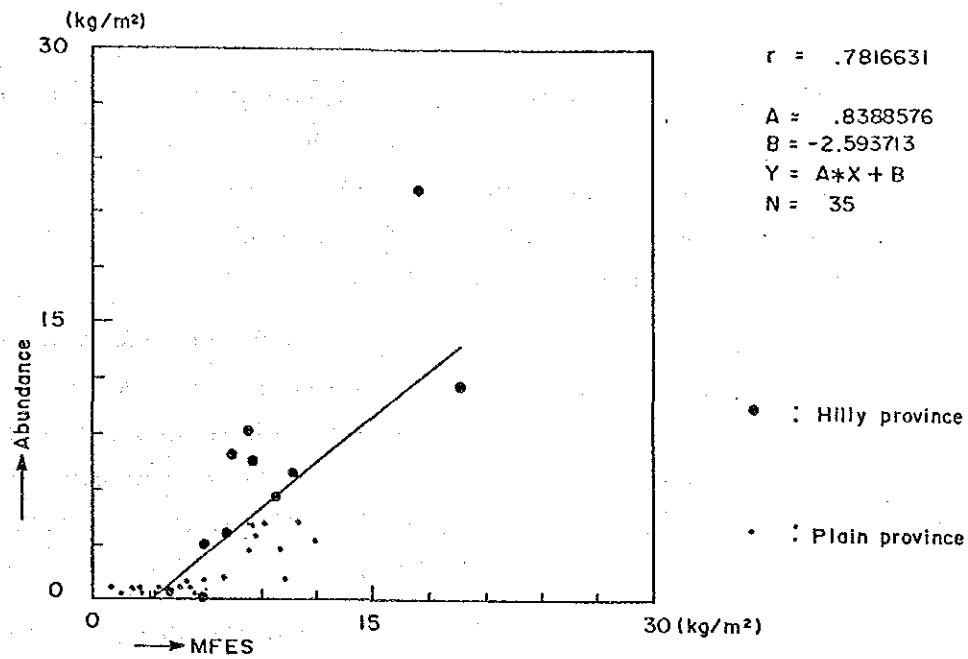


Fig. 4-4-5 Related Between MFES Intensity and Abundance of Manganese Nodule

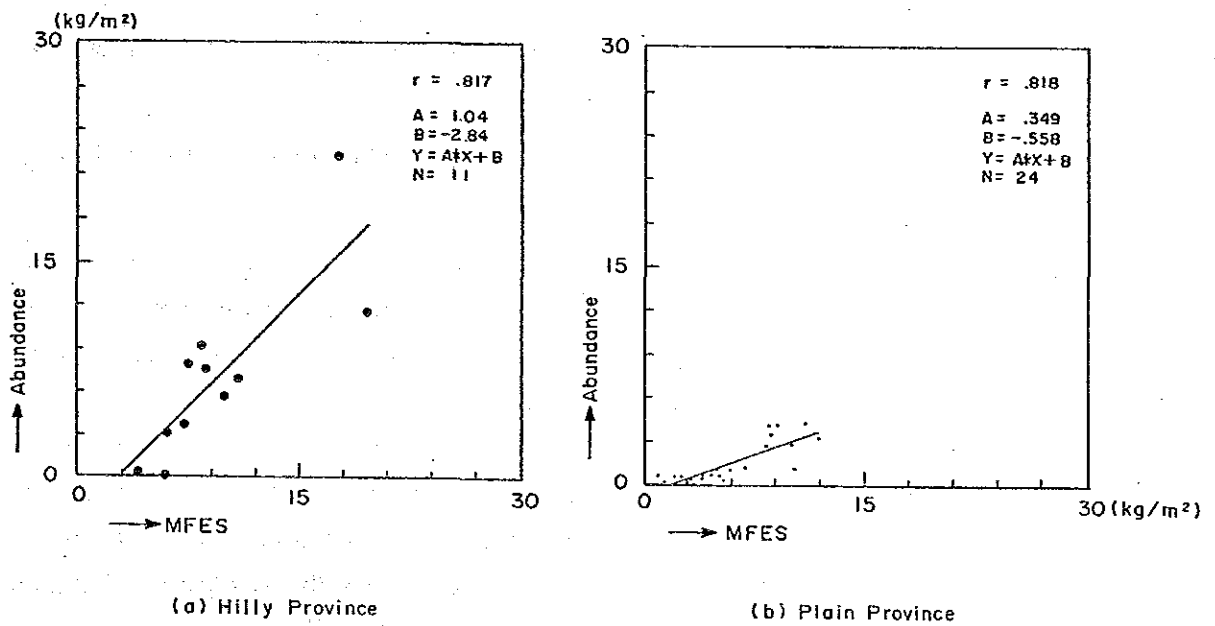


Fig. 4-4-6 Relation between MFES Intensity and Abundance of Manganese Nodules in Plain and Hilly Province

As shown in Fig. 4-4-6, the correlation coefficient for both hills and plains is more than 0.8. It is in good correlation, but the formula for both zones are greatly different:

Hills: Abundance = $1.05 \times \text{MFES value} - 2.84$

Plains: Abundance = $0.35 \times \text{MFES value} - 0.56$

That is to say: the coefficient on the plains becomes 0.35 (this is relatively small) and its MFES value is measured as a remarkably great one, while the MFES value on the hills is almost in proportion by 1:1 to the abundance of manganese nodules. This indicates that there is some cause of error on the plains which is impossible to correct using only the weight factor.

As in the SBP records in this survey areas, record types without an upper transparent layer which are distributed in a wide range (cf. Fig. 4-4-1), it is presumed that the reflection ratio in the area among *1 opaque layer becomes higher than that of the area among transparent layer.

That is to say, the MFES value is measured as higher than real abundance.

The distribution situation on the preceding plains is shown in Fig. 4-4-7 with indicated SBP record type.

As shown in Fig. 4-4-7, all the type b records indicate low distribution, while type C records which indicates an upper opaque layer show a distribution situation extremely higher than abundance of manganese nodules.

*1 It was not possible to perceive the difference the character of bottom materials among transparent layers and that of bottom materials among opaque layers from the results of the mud materials extracted by spade corer or other means.

It would be necessary on the next occasion to compare the results by spade corer and SBP record results with samplings taken by a piston corer with more than 10 m length of core samples.

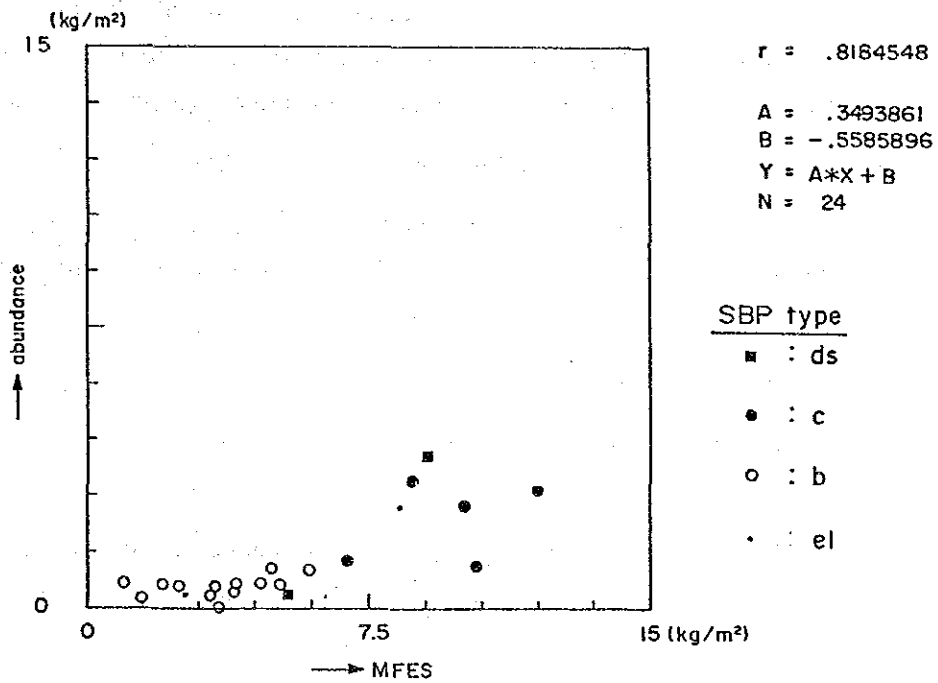


Fig. 4-4-7 Relation Between MFES Intensity and SBP Type

This makes us estimate that the great variety of regression coefficient on the plains dependant on the high reflection ratio of type C records. It was impossible to indicate type d2 records on the distribution situation diagram since stations were not perceived. On the topographical view type d2 records seem to be in a similar environment and tendency as type c records.

Therefore, it is highly probable that the area where type c and ds records are distributed is a quasi-anomaly area. In this survey, area analysis diagram by MFES was made after correction for this quasi-anomaly by using the above-mentioned regression formula.

2) Estimation of manganese nodules by means of MFES

Fig. 4-4-8 shows the estimated abundance of manganese nodules in the survey areas from the preceding results and according to the abundance by means of MFES.

This indicates as follows;

(1) The hills (West of the 159° W)

- Sea Area A

Abundance is over 10 kg/m², and it makes us estimate that this area bears a rather great amount of manganese nodules because of the extent and strength of abundance.

- Sea Area B

Abundance is between 5 and 8 kg/m², and this is also a promising area next to Sea Area A.

(2) The plains (East of the 159° W)

- Sea Area C

This is the area where SBP type C and d2 are distributed. This is a quasi-anomaly area with a great reflection ratio. Abundance is about 3 kg/m² estimated from the preceding results.

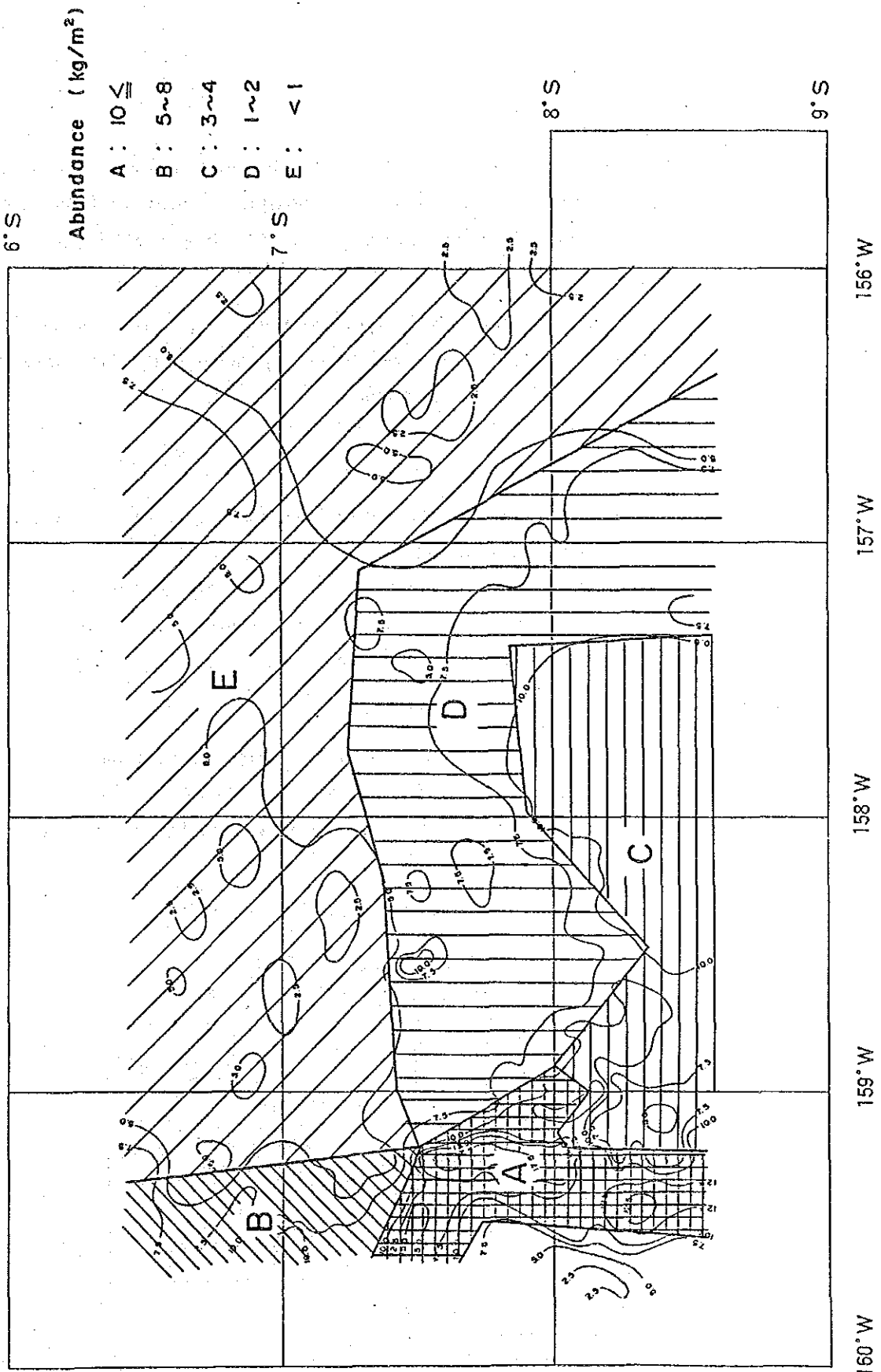


Fig. 4-4-8 Estimated High Potential Area by MFES Intensity

- Sea Area D

This area indicates SBP type el. Estimated abundance is 2 kg/m², and seems to have some possibility with an indication greater than 2 kg/m² around the sea knolls along 7°30' S line.

- Sea Area E

This area indicates SBP type b being rich with superficial sediment. Abundance is less than 1 kg/m² and this sea area is estimated to be a sterile zone.

4-5 Bottom Materials

Bottom materials on the survey area have two main groups: brown clay materials and calcareous sediments.

Calcareous sediments are distributed in the relatively shallow sea area adjacent to the sea mounts and on the sea knolls, while brown clay materials are distributed in the other areas.

1) Classification of bottom materials

Classification of bottom materials is done according to the classification criteria of bottom materials shown in Tab. 4-5-1. Quantitative analysis of each composition was made by the microscope observation using Smear slide (x-100).

Table 4-5-1 Classification Criteria of Bottom Sediment

	Fossil (%)	*1 Siliceous (%)	*2 Calcareous (%)	Remarks
Brown clay	<10			Contains zeolite minerals *1 more than 5 - 10%
Zeolitic clay	<10			
Insoluble brown clay	<10			Impermiabile
Silic-calcareous clay	10 - 30		> 5	Siliceous Fossil > Calcareous Fossil
Calc-siliceous clay	10 - 30	> 5		Calcareous Fossil > Siliceous Fossil
Calcareous clay	10 - 30	< 5		
Foraminifera	> 30			Calcareous Fossil > Siliceous Fossil, mainly foraminifera dominant

*1 Radiolaria, Diatoms, Silicoflagellate, Sponge Spicule

*2 Foraminifera, Calcareous Nannoplankton

*3 Phillipsite, Clinoptilolite

2) Properties of bottom materials

Fig. 4-5-1 shows major microscope pictures of each bottom material.

Properties of bottom materials are generally described in this section.

(1) Brown clay materials

① Brown clay

Brown clay in the survey area has mainly less than 5% of siliceous biogenic test content, and often contains nothing of siliceous biogenic test.

Its main component minerals are clay minerals and secondly siliceous creature shells which are mainly radiolarian test and diatom test.

Other remarkable minerals are zeolitic minerals and in general a small amount of spicule, pieces of clastics micro-nodule, ichthyolith and barite.

Its color is generally a dark brownish red (almost like chocolate brown). Its granular size is rather coarse (this seems to be because it contains zeolite) and it is insoluble.

② Zeolitic clay

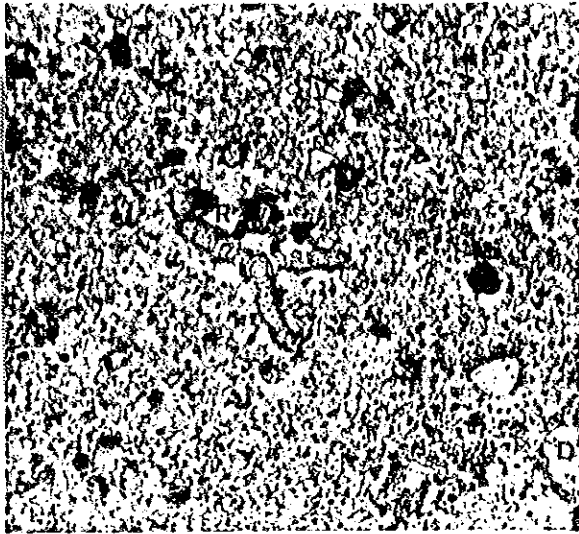
This is almost the same as brown clay, and is distinguished from brown clay only when its zeolitic content is over 5%.

In general, most brown clay materials in the survey area contain zeolitic minerals.

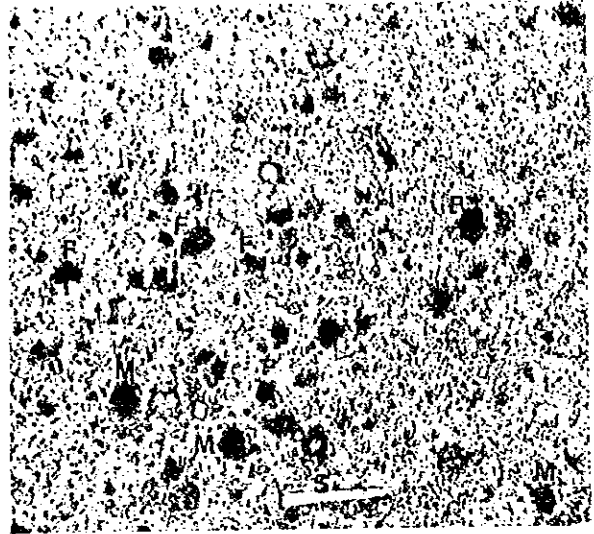
There was only sampling point where the sample contained over 5% of zeolitic minerals.

③ Insoluble brown clay

This is almost the same as brown clay. Its characteristics are a brownish yellow color (slightly lighter than brown clay), very fine grained with a great cohesion, as sticky as birdlime, and insoluble.



Brown clay
(85S739FG01)



Calcareous clay
(85S938FG08)

Legend

R : Radiolaria	D : Diatom	S : Sponge spicule
F : Foraminifera	V : Volcanic fragment	M : Mud fragment

Fig. 4-5-1 Smear Slide Photos of Bottom Sediments

The samples was taken a small quantity of mottles *1 in the brown clay obtained by the spade corer at one sampling point.

(2) Calcareous sediments

This is classified into 4 groups according to the quantitative ratio of siliceous biogenic debris and calcareous biogenic debris siliceous-calcareous clay, calcareous-siliceous clay, calcareous clay, foraminifera ooze.

There is little difference among the 4 groups except for that ratio. Their color is brown or dark brownish red being a little bit lighter than that of brown clay.

Their granular size is medium or coarse. Calcareous biogenic debris mainly consists of foraminifera pieces and other mineral components are almost the same as that of brown clay except for the smaller amount of zeolitic minerals.

3) Composing minerals of bottom materials

Composing minerals were investigated by X-ray diffraction analysis of powdered samples of bottom minerals and authigenic minerals.

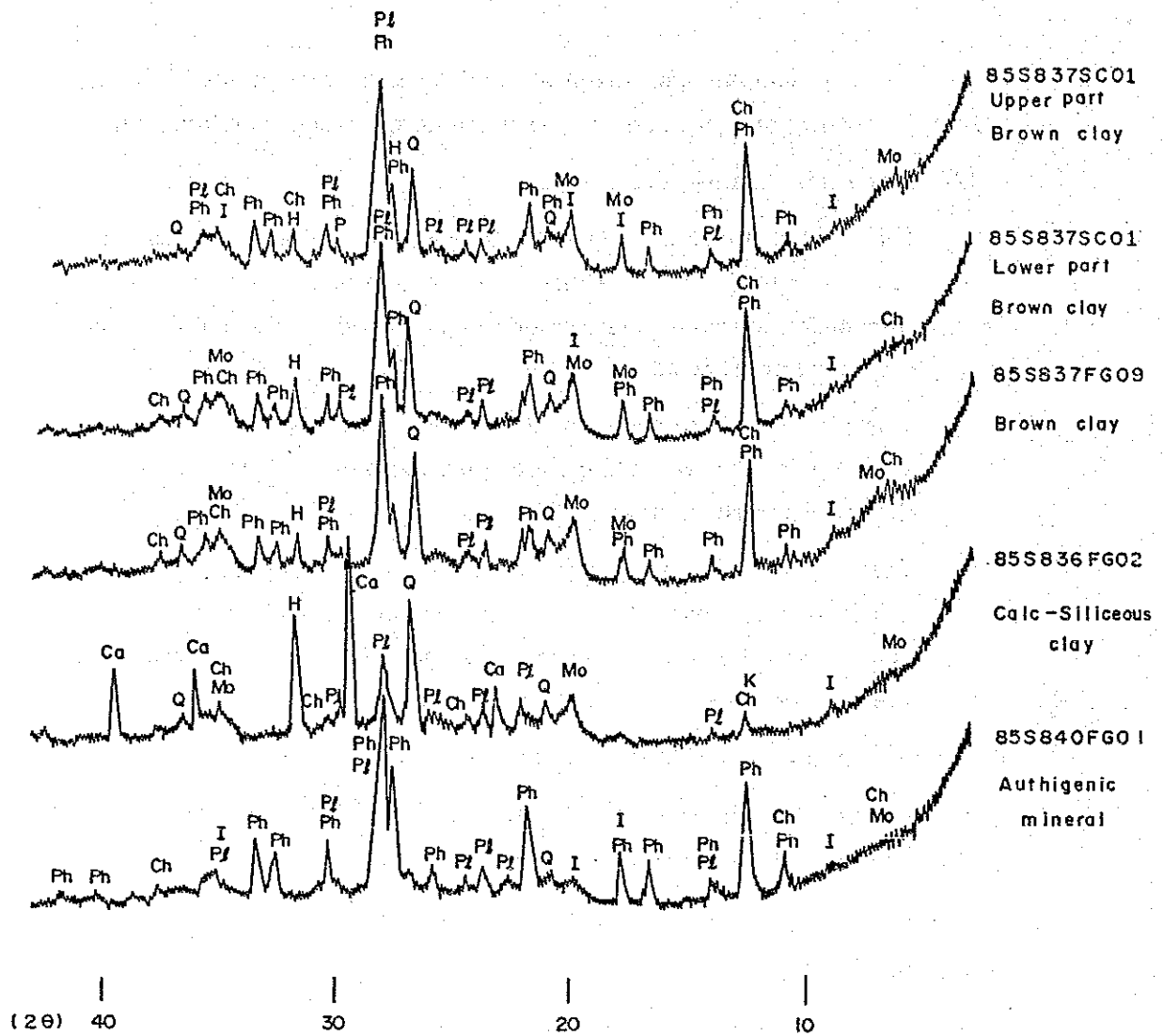
These results are shown in Tab. 4-5-2 and Fig. 4-5-2. *2

(1) Brown clay

Quartz, plagioclase, phillipsite and clay minerals were detected. Clay minerals are illite, montmoeillonite and kaolinite in extremely small quantities.

*1 Spots in different color of matrix which can be observed in the section of bottom materials.

*2 Authigenic minerals are described in section 5).



Legend

Q : Quartz Pz : Plagioclase I : Illite Mo : Montmorillonite Ch : Chlorite
 K : Kaolinite Ca : Calcite Ph : Phillipsite H : Halite

Fig. 4-5-2 Typical Pattern of the X-ray Diffraction of Bottom Sediment and Authigenic Mineral

Table 4-5-2 Results of X-ray Diffraction Analysis of Bottom Materials

Mineral Sample No.	Quartz	Plagioclose	Illite	Montmorillonite	Chlorite	Kashinite	Calcite	Phillipsite
85S837SC01 Upper Brown Clay	##	+	±	±	±	±		##
85S837SC01 Lower Brown Clay	##	+	±	±	±	±		##
85S837FG09 Brown Clay	##	+	+	±	+			##
85S836FG02 Calc- Siliceous Clay	##	+	±	±	±	±	##	
85S840FG01 Authogenic Minerals	+	+	±	±	±			##

* ## ## + means intensity of diffraction peaks in descending order

± means very weak diffraction peaks

Table 4-5-3 Chemical Composition of Bottom Materials

(Complete Analysis)

(%)

Sample No.	SiO ₂	TiO ₂	Al ₂ O ₃	Fe ₂ O ₃	FeO	MnO	MgO	CaO	BaO	Na ₂ O	K ₂ O	P ₂ O ₅	Ig-loss	Total
85S837SC01 Upper (Brown Clay)	44.08	0.92	13.59	10.04	<0.01	1.81	3.46	3.10	0.05	3.97	2.14	1.62	10.84	95.63
85S837SC01 Lower (Brown Clay)	44.03	0.94	13.43	9.94	<0.01	1.88	2.82	2.95	0.04	3.82	2.28	1.80	10.68	94.62

(Micro Analysis)

(%)

Sample No.	Pb	Zn	Ni	Cu	Co	Sr	V	Mo	B	As	Y
85S837SC01 Upper (Brown Clay)	0.007	0.016	0.032	0.053	0.017	0.024	0.010	0.004	0.032	0.002	0.032
85S837SC01 Lower (Brown Clay)	0.007	0.018	0.038	0.054	0.018	0.024	0.014	0.004	0.031	0.002	0.032

There are no variations of mineral component depending on the difference in depth from the sea bottom (the difference between data from the upper layer and data from the bottom layer sampled by means of SC).

Therefore, mineral component near the surface layer seems to have uniform distribution.

Brown clay in this surveyed area contains considerable phillipsite.

(2) Calcareous - siliceous clay

calcareous - siliceous clay was selected for samples of calcareous sediment.

Detected minerals are calcite, quartz, plagioclase, illite, montmorillonite, chlorite, and kaolinite and are characterized by a great amount of calcite.

4) Chemical composition of bottom materials

Chemical analysis was done ashore for bottom materials sampled by spade corer (SC) being grouped into upper and lower materials. Tab. 4-5-3 shows the results of the analysis. In comparison with the chemical composition *1 of bottom materials on DOMES Site-B by Peris, bottom materials in this sea area have higher content of TiO_2 , Al_2O_3 , Fe_2O_3 , MnO , CaO and P_2O_5 especially with a higher content of MnO and CaO . On the other hand bottom materials in this sea areas have a lower content of SiO_2 , Na_2O , K_2O and Ig-loss.

There is no great difference between the content of upper bottom materials and that of lower bottom materials in this sea area having a lower content of MgO among lower bottom materials than that of upper bottom materials.

5) Rocks of bottom materials

Among samples from the surveyed area there were no rocks and only a small amount of authigenic minerals.

*1 SiO_2 51.5%, TiO_2 0.59%, Al_2O_3 12.5%, Fe_2O_3 5.4% MnO 0.53%,
 MgO 3.0%, CaO 1.5%, Na_2O 5.7%, Ig-loss 11.2%

X-ray diffraction analysis was done on some powdered samples selected from the authigenic minerals (Refer to Tab. 4-5-2 and Fig. 4-5-2), and observation by microscope was done on these samples (Refer to Fig. 4-5-3).

Authigenic minerals have brownish red, dark brown, and black in color, and have shapes of semi-fragment, plate, bark, twig and lump with a lot of small granules (about 0.5 cm on an average and 2 cm at a maximum in diameter). On the X-ray diffraction chart, there are characteristics of phillipsite and also other minerals such as quartz, plagioclase, illite, montmorillonite and chlorite. A lot of dispersed mineral fragments among the clay matrix can be observed by microscope with growing manganese oxides having the shape of bark and small veins or with a growing fish egg-like texture appearing to be corpses of creatures. Authigenic minerals with a growing fish egg-like texture have characteristics of clay and partial crystallisation of zeolite within their texture.

From the result of X-ray diffraction analysis the authigenic minerals seem to be aggregates of zeolitic minerals (mainly phillipsite), clay minerals, mineral fragments and corpses of creatures.

6) Distribution of bottom materials

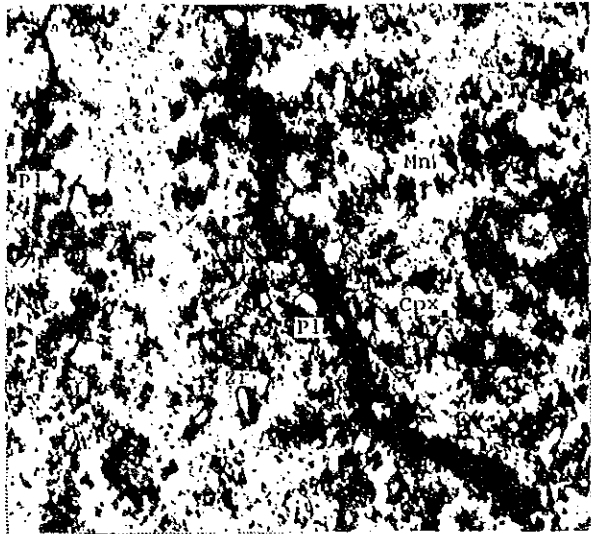
Distribution situation of the bottom materials is shown in Fig. 4-5-4.

① Brown Clay Materials

The recovery of brown clay materials from total bottom materials sampled is 94.4%. This indicated that the major component of bottom materials in the survey area is brown clay. Comparing the zeolitic mineral content, the eastern part of south ridge in the survey area has 1% of zeolitic minerals, and has a smaller zeolitic mineral content than the other parts of the survey area.

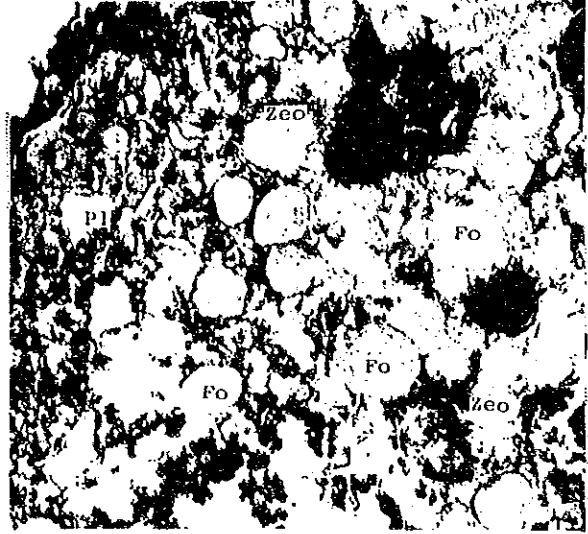
② Calcareous sediment

The recovery of calcareous sediment is 5.6%, and these materials are distributed in relatively shallow place around the sea knoll and



open nicol

0 0.5mm



open nicol

0 0.5mm

(85S840FG01)

open nicol

Legend

Mn : Manganese oxide Pl : Plagioclase Cpx : Clinopyroxene
 Zr : Zircon Zeo : Zeolite minerals Fo : Fossil fragment

scale bar : 0.5 mm

Fig. 4-5-3 Microscopic Photos of Authigenic Minerals

sea mount according to the calcium carbonate compensation depth (CCD). In the survey area these sediments are distributed in the central part, the western ridge, and the western part of the south ridge, and their CCD estimated to be between 5,000 and 5,200 m.

③ Authigenic mineral nodules

Fig. 4-5-4 shows the distribution situation of the authigenic mineral nodules.

This indicates that authigenic mineral nodules are distributed in a slightly greater amount in the western part of the survey area.

7) Identification of micro-fossils in bottom sediments

Identification of fossils (Radiolaria) in bottom materials samples by spade corer was done with 2 samples selected from the bottom materials including samples at the points of 0 cm, 10 cm and 20 cm from the surface of bottom materials (namely 6 samples in total). Radiolarias occurring in the surveyed areas are shown in Tab. 4-5-4 and Tab. 4-5-5, and photographs of the species of Radiolaria are shown in Fig. 4-5-5 and 4-5-6.

① Fossils situation

Samples No.: 85S837SC01

0 cm: Many fossils as well as many different species in a good state of preservation were found.

10 cm: Many fossils as well as many different species were found but not as many as at the 0 cm level.

The preservation is also worse.

20 cm: No occurrence of Radiolaria. The only fossils found were Ichthyoliths.

Samples No.: 85S937SC01

0 cm: Many fossils as well as many different species in a good state of preservation were found. In comparison with 0 cm case of sample No.: 85S837SC01, the Radiolarian frame melting condition is slightly better.

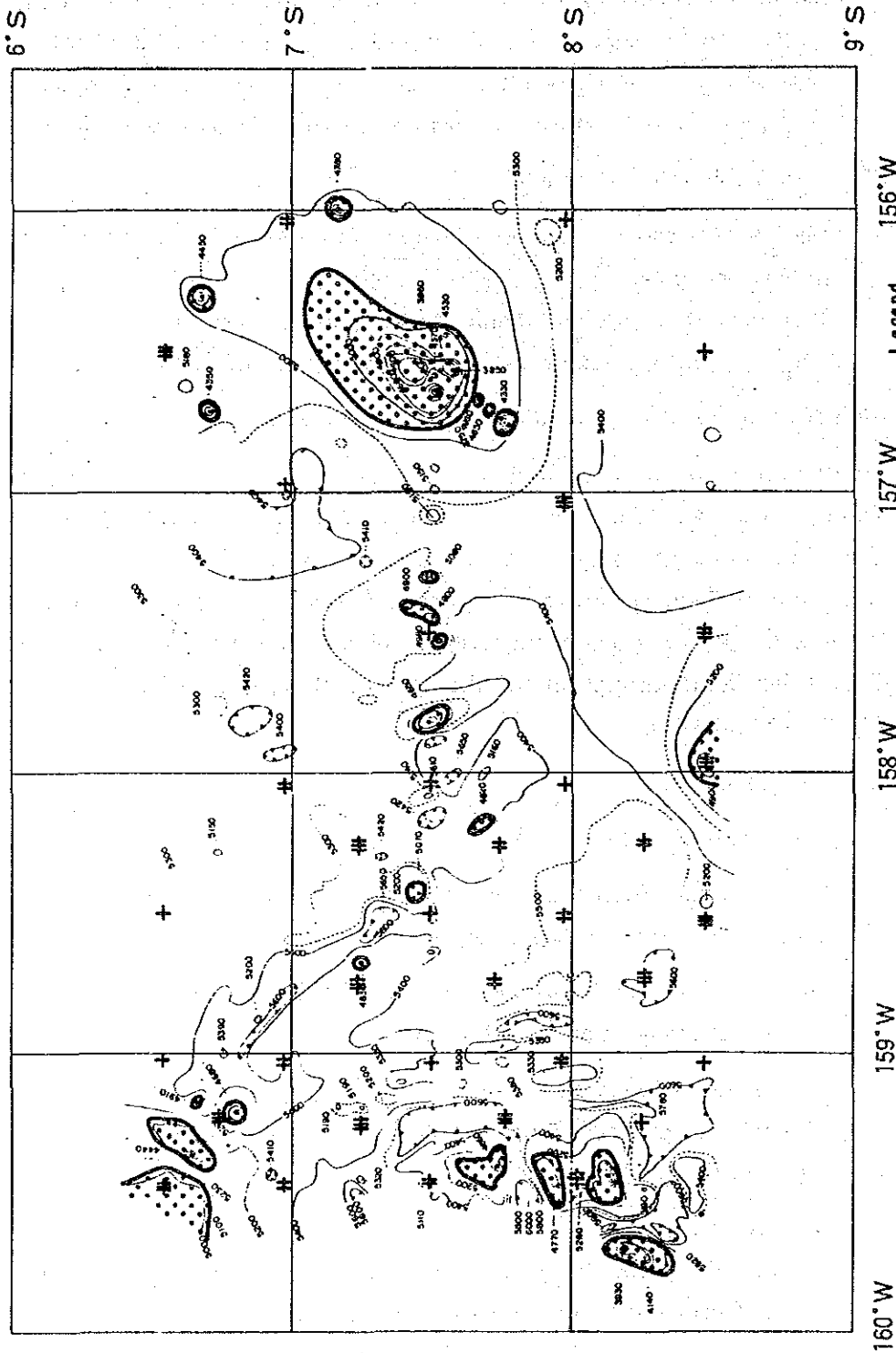
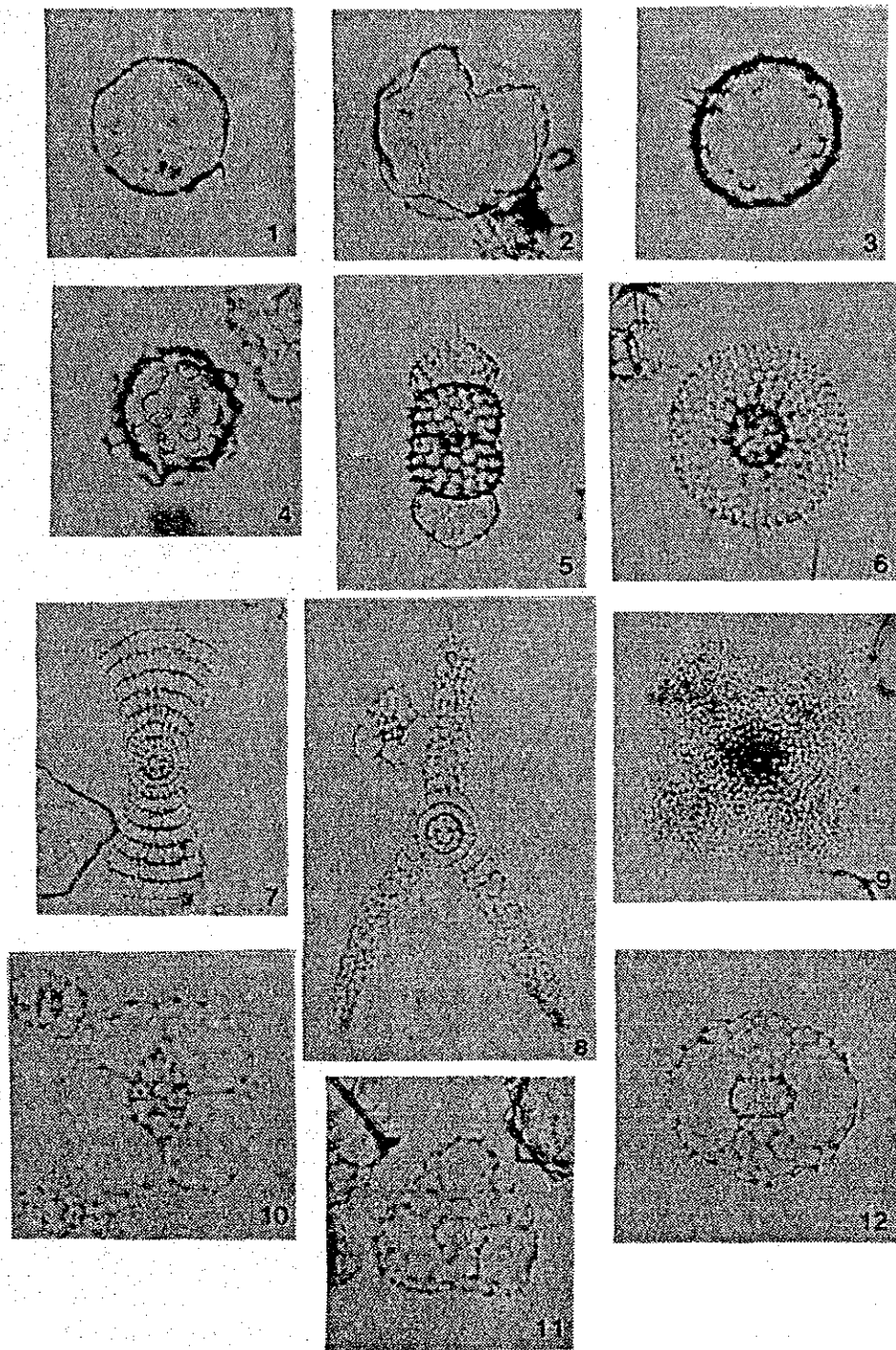
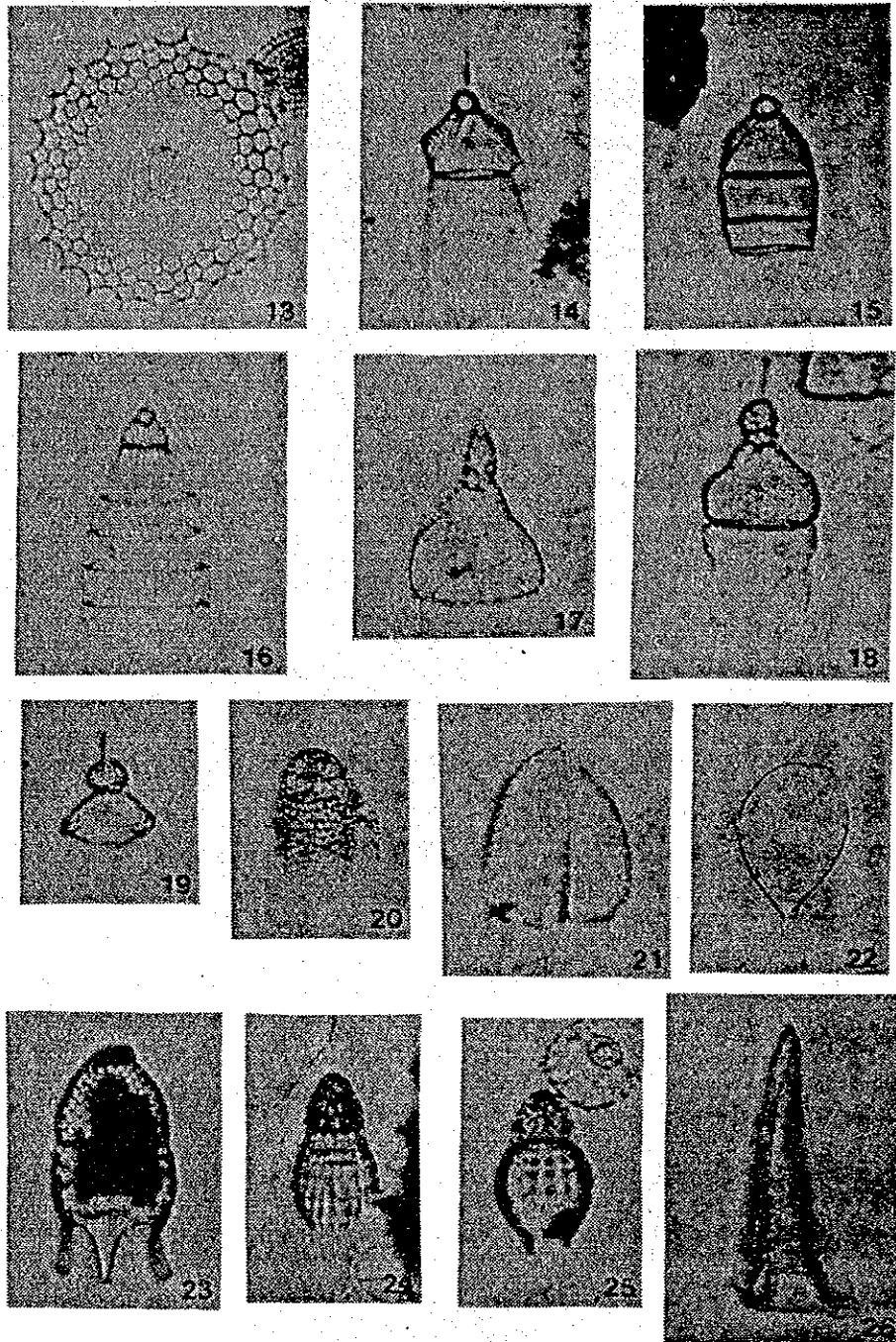


Fig. 4-5-4 Distribution of Bottom Materials



- | | |
|---|---|
| 1 <i>Buccinosphaera invaginata</i> Haeckel | 7 <i>Amphirhopalum ypsilon</i> Haeckel |
| 2 <i>Collosphaera tuberosa</i> Haeckel | 8 <i>Eucitonia elegans</i> Ehrenberg |
| 3 <i>Acrosphaera lappacea</i> (Haeckel) | 9 <i>Spongaster tetras tetras</i> Ehrenberg |
| 4 <i>A. murrayana</i> (Haeckel) | 10 <i>Larcospira quadrangura</i> Haeckel |
| 5 <i>Ommatartus tetrathalamus tetrathalamus</i> (Haeckel) | 11 <i>Hexapyle dodecantha</i> Haeckel |
| 6 <i>Heliodiscus asteriscus</i> Haeckel | 12 <i>Tetrapyle octacantha</i> Muller |
- Magnification x 150

Fig. 4-5-5 Species of the Typical Radiolarian Fossil (No. 1)



- | | |
|--|---|
| 13 <i>Lampromitra butschlii</i> (Haeckel) | 20 <i>Botryocyrtis scutum</i> (Harting) |
| 14 <i>Pterocanium praetextum</i> (Ehrenberg) | 21 <i>Nephrospyria renilla</i> Haeckel |
| 15 <i>Eucyrtidium anomalum</i> (Haeckel) | 22 <i>Zigocircus capulosus</i> Popfsky |
| 16 <i>E. dictyodium</i> (Haeckel) | 23 <i>Thyrsocyrtis rhyzodon</i> Ehrenberg |
| 17 <i>Anthocyrtidium ophirense</i> (Ehrenberg) | 24 <i>Dictyoprora amphora</i> (Haeckel) |
| 18 <i>Theocorythium trachelium</i> (Ehrenberg) | 25 <i>D. mongolfieri</i> (Haeckel) |
| 19 <i>Clathrocanium reginae</i> Haeckel | 26 <i>Ichthyoliths</i> |

Magnification x 150

Fig. 4-5-6 Species of the Typical Radiolarian Fossil (No. 2)

10 cm: There are few Radiolaria in preservation with frame damage and slight melting.

20 cm: No occurrence of Radiolaria. The only fossils found are Ichihyoliths.

② Time classification

Of the frequently found species of Radiolaria in the 3 samples, all are in existence at the present except for 3 species in the latter 3 rows of Tab. 4-5-4 and Tab. 4-5-5.

There are no *Stylocentron acquilonium* (Hays), *Axoprunum angelinum* (Campbell et Clark) and *Amphirhopalum praeypilon* Sakai which were extinct during the latter period of the Quaternary (about 400,000 years ago), but there are *Collosphaera tuberosa* Haeckel and *Amphirhopalum ypsilon* Haeckel which still exist and have existed since the latter part of the Quaternary period. Among the top layers of the 2 cored samples there are *Buccinosphaera invaginata* Haeckel which occurred 200,000 years ago.

According to these facts the top layers of cored samples are probably today's new sediment which did not exist 200,000 years ago.

Observing the fossils in the 10 cm level (sample No. 85S837SC01) their age is estimated between 200,000 and 400,000 years old for the reason that they do not contain *B. Invaginata*; however, as the frame of *B. Invaginata* is particularly more soluble than others, there remains some possibility that it could not be found at the 10 cm level because it had disappeared by the soluble action existing there and could not be observed by means of a microscope. (That is to say, younger than 20,000 years old)

Radiolarians occurring in the 10 cm level sample No. 85S967SC01 are the species occurring often in the upper layer.

Table 4-5-4 List of the Collected Radiolarias (No. 1)

Species	Sample No.	85S837SC01			85S937SC01		
		0cm	10cm	20cm	0cm	10cm	20cm
Acrosphaera flammabunda (Haeckel)		X	X		X		
A. lappacea (Haeckel)		X	X		X		
A. murrayana (Haeckel)		X	X		X		
Buccinosphaera invaginata Haeckel		X			X		
Collosphaera huxleyi Muller		X	X		X		
C. tuberosa Haeckel		X	X		X		
Otosphaera polymorpha Haeckel		X	X		X		
Siphonosphaera socialis Haeckel		X	X		X		
Acanthosphaera capillaris Haeckel		X	X		X		
Actinomma archadophorum Haeckel		X					
A. spp.		X	X		X		
Actinosphaera capillacea (Haeckel)		X					
Amphisphaera cf. palliatum (Haeckel)		X					
Druppactructus spp.		X	X		X		
Hexacontium elegans (Haeckel)		X	X		X		
H. heracliti (Haeckel)		X	X		X		
H. hostile Cleve		X	X		X		
H. hexacanthum (Muller)		X	X		X		
H. sp.		X					
Hexacontarium sp.		X	X		X		
Stylatractus melpomene (Haeckel)		X	X		X		
S. cf. neptunus Haeckel		X	X		X		
Thecosphaera radianus Holland et Enjume		X			X		
Xiphatractus sp.		X	X		X		
Ommatartus tetrathalamus tetrathalamus (Haeckel)		X	X		X	X	
Heliodiscus asteriscus Haeckel		X	X		X	X	
Amphirhopalum ypsilon Haeckel		X	X		X		
Eucitonia elegans Ehrenberg		X	X		X		
E. frucata Ehrenberg		X	X		X	X	
Dictyocoryne profunda Ehrenberg		X	X		X	X	
D. truncatum (Ehrenberg)		X	X		X		
Spongaster tetras tetras Ehrenberg		X	X		X		
Spongocore cylindrica (Haeckel)		X			X		
Spongodiscus biconcavus Ehrenberg		X	X		X		
S. osculosus (Dreyer)		X	X		X		
Stylodictia spp.		X	X		X	X	
Xiphospira spp.		X	X		X		
Larcopyle lutschlii Dreyer		X	X		X		
Larcospira quadrangura Haeckel		X	X		X		
Hexapyle dolecantha Haeckel		X	X		X		
Tetrapyle octacantha Muller		X	X		X	X	

Table 4-5-5 List of the Collected Radiolarias (No. 2)

Species	Sample No.	85S837SC01			85S937SC01		
		0cm	10cm	20cm	0cm	10cm	20cm
Clathromitra pentacantha Haeckel		X	X		X		
Clathrocanium reginae Haeckel		X	X		X		
Pseudodictyophimus glacilipes (Bailey)		X	X		X		
Lampromitra butschlii (Haeckel)		X	X		X		
Botryocyrtis scutum (Harling)		X	X		X		
Carpocanium spp.		X	X		X	X	
Eucecryphalus elizabethae (Haeckel)		X	X		X		
Eucyrtidium acuminatum Ehrenberg		X	X		X		
E. anomalum (Haeckel)		X	X		X	X	
E. dictyopodium (Haeckel)		X	X		X		
Lipmanella bombus (Haeckel)		X			X		
L. virchovi (Haeckel)		X	X		X		
Dictyophimus infabricatus Nigrini		X	X		X		
Pterocanium charibdeum (Muller)		X	X		X		
P. praetextum (Ehrenberg)		X	X		X		
P. trilobium (Haeckel)		X	X		X	X	
Anthocyrtidium ophirense (Ehrenberg)		X	X		X		
A. zanguebaricum (Ehrenberg)		X	X		X		
Lamprocyclas maritalis Haeckel		X	X		X		
Lamplocyrtis gamphonycha (Jorgensen)		X	X		X		
Pterocorys hertwigii (Haeckel)		X	X		X		
P. macroceras (Popofsky)		X	X		X		
P. zancleus (Muller)		X	X		X		
Theocorythium trachelium (Ehrenberg)		X	X		X		
Botryostrobus aquilonaris (Bailey)		X	X		X	X	
B. auritus (Ehrenberg)		X	X		X		
Phrmostichoartus corbula (Harling)		X	X		X		
Spirocyrtis scalaris Haeckel		X	X		X		
S. subscalaris Nigrini		X	X		X		
Tholospyris ramosa Haeckel		X	X		X		
T. acuminata (Hertwig)		X	X		X	X	
Acanthodesmia vuniculata (Muller)		X	X		X	X	
Liriospyris reticulata (Ehrenberg)		X	X		X		
Nephropsyris renilla Haeckel		X			X		
Zigocircus capulosus Popofsky		X	X		X		
Thyrsocyrtis rhyzodon Ehrenberg			X				
Dictyoprora amphora (Haeckel)		X					
D. mongolfieri (Ehrenberg)			X				
Ichthyoliths			X	X		X	X

As there are a few Radiolarias which are rather easy to be melted and damaged, Radiolarias occurring in the upper layer seem to be mixed with those in the lower layer.

The ages of 3 samples with a small amount of Radiolarian occurrence or without its occurrence could not be made clear.

③ Miscellaneous

Each of the above-mentioned 3 species of fossils found in sample No. 85S837SC01 existed in the middle period of the Eocene period during Tertiary. On every sea bottom in the Pacific Ocean there are such phenomena that the more ancient species of fossils are mixed within other species of fossils which occurred in the latter half of Quaternary or the present period.

Furthermore, it is known that the ancient sediment are directly exposed or dispersed in a rather shallow areas around the sea bottom where these phenomena (Hiathas phenomena) occur.

Therefore, such phenomenon can be assumed to occur adjacent to the core-sampled areas.

4-6 Sea Bottom Observation

Sea bottom observation in the surveyed areas for this financial year was done by photographing the sea bottom surface by CDC intermittently and by deep-sea camera mounted on FG and SC.

1) Observation by CDC

Observation by CDC was done from 8:00 on October 19th until 13:30 on October 22nd for 77 and half hours after finishing the secondary sampling.

During this investigation photographing of 3 lines, 64.56 nautical miles in total length, and 41 observation stations was executed, and 168 pictures of the sea bottom were taken.

(1) Results of observation (cf. Annexed Fig. 6)

Annexed Fig. 6 shows the CDC observation stations and results with an average ^{*1} abundance (kg/m²) which is calculated from the deep-sea photos on the topographical map of the surveyed areas.

According to this figure, the distribution situation of manganese nodules has a continuous rate of variation on the extend margin of the Manihiki plateau; but in the areas with intensely undulated topography, especially in the vicinity of top of sea mounts, a great variation was observed in distribution of manganese nodules in an extent of only 500 meters along the track line.

① Track line No.1

The line starts at the station of 8° 00'S: 159° 30'W and ends at the station of 7°44'S: 159°14'W. Its distance is 22.40 nautical miles with 18 stations having 1.33 nautical miles distance between each of them. The south-western part (about 2/3 of the line) has greatly varying topography ^{*2} with relative height changing within + 830 m.

The east-northern part (about 1/3 of the line) has relatively flat topography with a small inclination towards the final station.

Abundance per station by photo-analysis is 1.30 kg/cm² at a minimum and is 25.08 kg/cm² at a maximum.

*1 Basic data for the calculation of abundance (kg/m²) and average granular size (cm) were obtained by calculating the coverage and the number of manganese nodules per m² in each photo.

*2 Basement rocks and clastics in photos by CDC indicate the remarkable variation of the sea bottom situation.

Stations which indicated low abundance, less than 7.5 kg/cm^2 are 5: from No. 1 to No. 4 and No. 14 about 16 nautical miles from the starting station.

The other 13 stations indicate a high abundance of 15-25 kg/m^2 .

The average abundance of the 18 stations is 17.77 kg/cm^2 which is a 15.45 surplus comparison with an average abundance of 15.03 kg/cm^2 for the sampling points of the secondary survey, (The secondary survey area contains 2 stations).

Abundance determined by MFES is on the whole concordant with the survey result by CDC.

The size of the manganese nodules at each station is 2.0 cm at a minimum, 5.4 cm at a maximum, and 3.6 cm on an average, with most granules being less than 4.5 cm in lengthwise diameter.

② Track Line No.2

The line starts at the station of $7^{\circ}30'S: 159^{\circ}30'W$, and ends at the station of $7^{\circ}45'S: 159^{\circ}15'W$.

Its distance is 21.08 nautical miles with 17 stations having 1.3 nautical miles distance between each.

At the starting station the depth is about 5,350 m, and decreases gradually toward the southeast part of the line. At station No.6, about 8 nautical miles from the starting station the depth is about 5,150 m at a minimum. The depth increases gradually from this station and is 5,400 m between stations No. 14 and No.15 with an acute increase up to 5,600 m within a distance of only 0.7 nautical miles. This depth continues up to position No.16, and then decreases again toward the end station being about 5,550 m at the end station.

Abundance per station by photo-analysis is 3.88 kg/m² at a minimum and 29.10 kg/m² at a maximum.

The abundance at station No.3 is 3.88 kg/m² which is the only station less than 7.5 kg/m².

Abundance in most positions is more than 15 kg/m² except in three stations (from No.1 to No.3) which have less than 10 kg/m² of abundance.

From station No.15 to No.17 a high abundance of more than 20 kg/m² is indicated. Average abundance at 17 stations is 16.27 kg/m² and 3.8% more than 15.65 kg/m² of the average abundance at 2 sampling points of the secondary survey areas containing 2 stations. Abundance determined by means of MFES is slightly less than that of photo-analysis, and there is good concordance with each other on the whole.

Size of manganese nodules in each station is 2.7 cm at a minimum, 4.7 cm at a maximum, and 3.6 cm on an average, composed with most granules being less than 4.5 cm in lengthwise diameter the same as track line No.1.

③ Track line No.3

This line starts at the station of 7°45'S: 159°15'W, and ends at the station of 8°00'S: 159°00'W.

Its distance is 21.08 nautical miles with 6 stations.

The distance between the first and second station is 1.33 nautical miles, and the distance between the second and third station is 2.65 nautical miles.

Distance between another stations is 5.3 nautical miles. Reason for selecting these distances is that the variation of the abundance of manganese nodules on the flat topography is smaller than that on the complicated topography within the margin of Manihiki plateau as determined by the sampling for the first and second stage survey and MFES.

At the starting station the depth is about 5,550 m, and gradually decreases toward the southeast on the line. At a point, 12 nautical miles from the starting station, the depth is about 5,350 m, and changes a little bit being almost flat topography up to the end station.

Abundance per station by photo-analysis is 1.85 kg/m^2 at a minimum, and 18.47 kg/m^2 at a maximum.

The station No.1 was omitted from the photo-analysis because in the photography of the station No.1 no shutter sinker can be seen.

On calculating an average abundance on the whole track line No.3, primarily, the value of the starting station was determined by an average of the abundance of station No.17 (track line No.1): 25.08 kg/m^2 and that of station No.17 (track line No.2): 20.22 kg/m^2 ; secondly, the standard interval distance between stations being 5.3 nautical miles, the mean value of abundance at station No.2: 18.47 kg/m^2 weighted as $1/2$; the average abundance thus calculated came to 13.44 kg/m^2 which is 9.4% less than the average abundance of 2 samples by FG sampling: 14.84 kg/m^2 .

Abundance on this track line by means of MFES on the whole has good concordance with the result of the photo-analysis. The size of manganese nodules per station is 2.9 cm at a minimum, 3.6 cm at a maximum and 3.3 cm on an average with most of the manganese nodules being nearly same size.

Therefore, the bearing situation of manganese nodules at the intensive distribution zones of the surveyed areas was clarified as shown in the annexed figure.

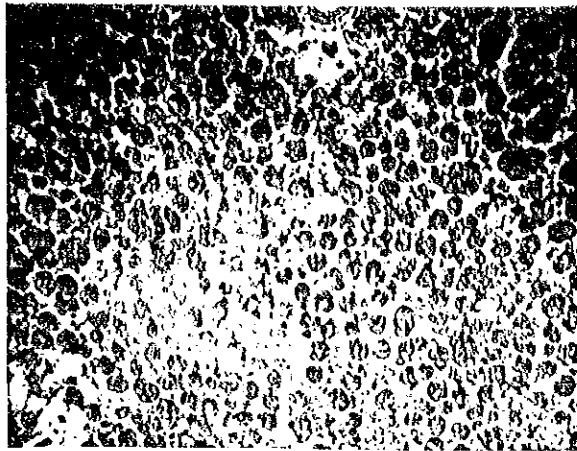
Fig. 4-6-1 shows a typical example of the sea bottom situation recorded by CDC.

2) Observation by deep-sea camera

The deep-sea camera was used by mounting it on samplers like FG and SC in order to get information about the bearing situation of manganese nodules and the general condition of the deep-sea bottom, and to produce basic data for calculating the abundance by CDC photography.

The morphology of manganese nodules in this survey area taken by photography are mainly flat-oval, and some of them are nuggets and sphere shaped. There are many exposed-type manganese nodules on the complicated topography of the sea bottom which is on the western side of longitude 159°W and on the margin of Manihiki plateau.

There are many photos of embedded or half-embedded manganese nodules on the flat topography of the sea floor which is on the eastern side of longitude 159°W. There are also some photographs of basement rock, rock pieces, and clastics thinly covered by manganese nodules on the adjacent sides toward the top of sea mounts and sea knolls. Fig. 4-6-2 and Fig. 4-6-3 show some typical examples of photography presenting the difference among bottom materials and presenting basement rock.

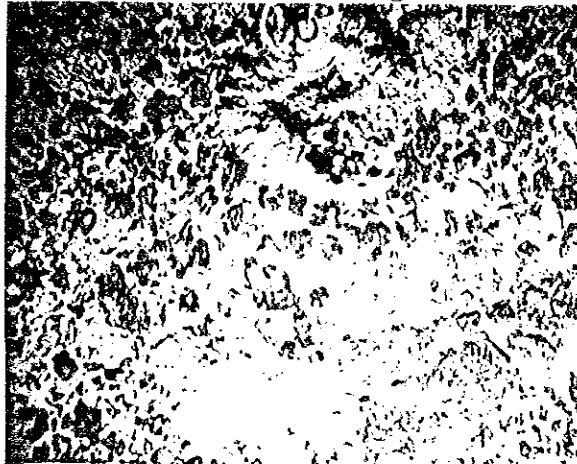


1985. 10. 20

85SCDC01 Point № 9

Example of high abundance of manganese nodules

Abundance: 29.05 kg/m²



1985. 10. 22

85S CDC 03 Point № 6

Example of low abundance of manganese nodules

Abundance: 1.93 kg/m²



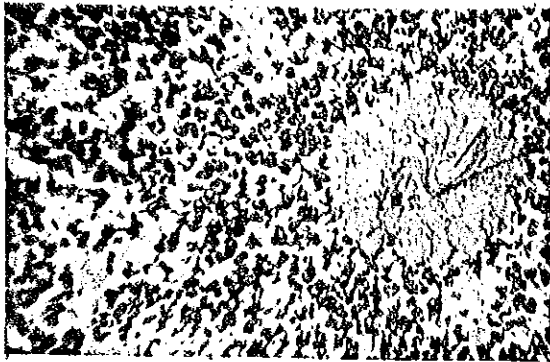
1985. 10. 20

85S CDC 01 Point № 9

Example of rocks exposed on sea bottom

Fig. 4-6-1 Examples of Photos by CDC

Sea-bottom photo

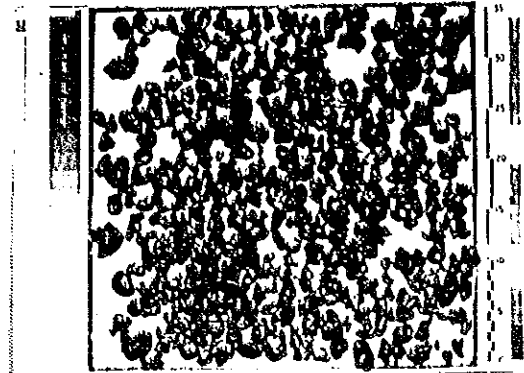


1985. 10. 1

85S836FG02

Exposed type manganese nodules

Re-collected samples photo



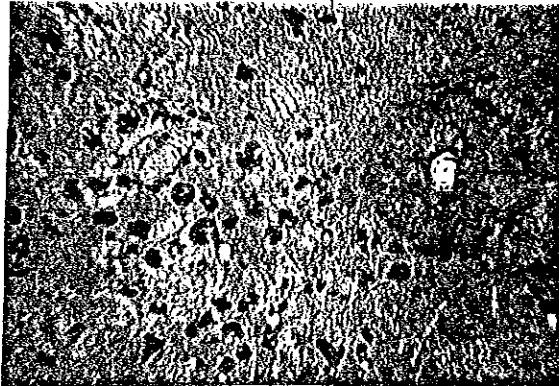
1985. 10. 1

85S836FG02

Morphology: Pebble thin and ellipsoidal

Abundance: 13.18 kg/m²

Sea-bottom photo

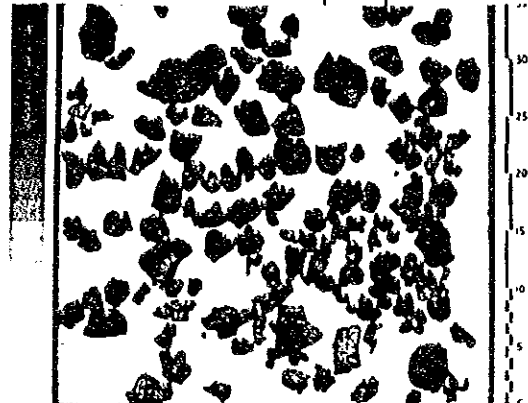


1985. 10. 1

85S836FG03

Half embedded type manganese nodules

Re-collected samples photo



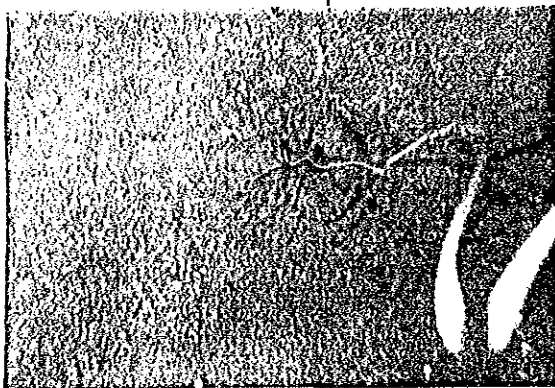
1985. 10. 1

85S836FG03

Morphology: Ellipsoidal and plate

Abundance: 8.43 kg/m²

Sea-bottom photo

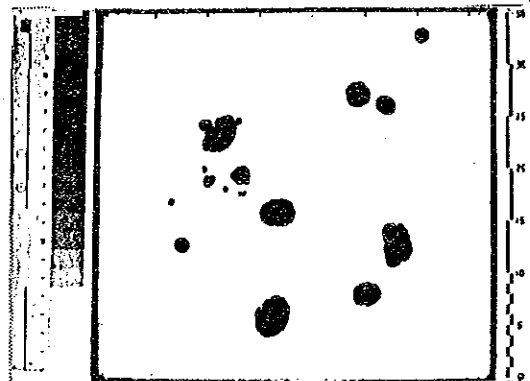


1985. 10. 17

85S737FG04

Embedded type manganese nodules

Re-collected samples photo



1985. 10. 17

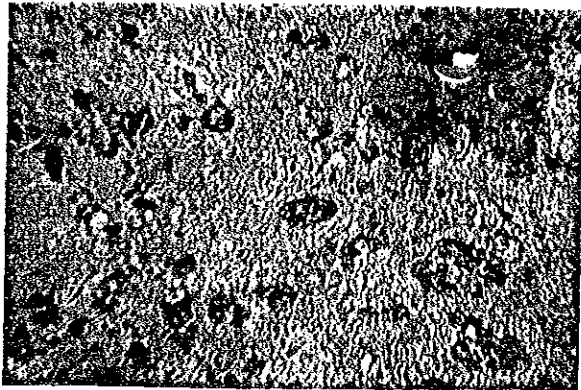
85S737FG04

Morphology: Ellipsoidal and pebble thin

Abundance: 4.6 kg/m²

Fig. 4-6-2 Examples of Deep-Sea Bottom Photos and of Re-collected Photos
(No.1)

Sea-bottom photo



1985. 9. 30

85S736FG01

Crusts and rock fragments

Abundance: 3.27 kg/m²

Re-collected samples photo

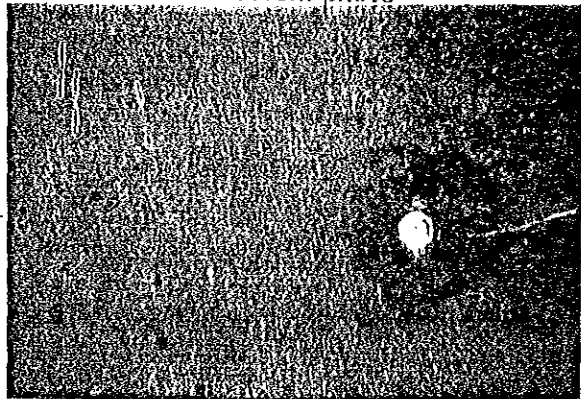


1985. 9. 30

85S736FG01

Morphology: Crust, rock fragments, massive plate

Sea-bottom photo



1985. 10. 11

85S936FG07

Brown clay

Abundance: 0.00 kg/m²

Sea bottom photo



1985. 10. 8

85S839FG05

Exposed rocks near top of sea knoll

Abundance: 0.00 kg/m²

Fig. 4-6-3 Examples of Deep-Sea Bottom Photos and of Re-collected Photos (No.2)

